



The fluid geochemistry of Ölkelduháls and Hveragerði geothermal areas – SW Iceland

Yerko Figueroa Peñarrieta



Faculty of earth science
University of Iceland
2021

The geochemistry of geothermal fluids of Ölkelduháls and Hveragerði geothermal areas, SW Iceland

Yerko Figueroa Peñarrieta

60 ECTS thesis submitted in partial fulfillment of a
Magister Scientiarum degree in Geology

MS Committee
Andri Stefánsson
Finnbogi Óskarsson

Master's Examiner
Þráinn Friðriksson

Faculty of Earth Science
School of Engineering and Natural Sciences
University of Iceland
Reykjavik, June 2021

The fluid geochemistry of Ölkelduháls and Hveragerði geothermal areas – SW Iceland
60 ECTS thesis submitted in partial fulfillment of a *Magister Scientiarum* degree in
Geology

Copyright © 2021 Yerko Figueroa Peñarrieta
All rights reserved.

Faculty of Earth Science
School of Engineering and Natural Sciences
University of Iceland
Sturlugata 7
101, Reykjavík
Iceland

Telephone: 525 4000

Bibliographic information:

Yerko Figueroa Peñarrieta, 2021, *The geochemistry of geothermal fluids of Ölkelduháls and Hveragerði geothermal areas, SW Iceland*, Master's thesis, Faculty of Earth Science, University of Iceland, pp. 66.

Printing: Háskólaprent Ltd.
Reykjavík, Iceland, September 2021

Abstract

The surface geothermal water and steam vent chemistry of the Hveragerði and Ölkelduháls geothermal areas SW Iceland were studied. In total 43 samples were collected of cold springs and rivers, hot springs, and steam vent discharges and their chemical composition analyzed.

The chemical composition of geothermal waters at surface was characterized by mildly acid to alkaline pH of 6.06-8.69 and low Cl concentration of 3.32-7.34 ppm and with SiO₂ and CO₂ generally being the most important dissolved elements with concentration of 38.5-217 and 6.43-486 ppm, respectively. Surface geothermal fluids are considered to be sourced from three end-member waters and mixture of: (1) boiled reservoir liquid, (2) condensed steam and (3) non-thermal water. Relationship between Cl, CO₂, SO₄ and temperature show evident signatures that surface geothermal fluids in the area are dominantly steam-heated waters with variable mixing ratios between condensed steam and non-thermal waters. No boiled reservoir liquids were observed at surface, these considered to represent boiled liquid fraction of reservoir geothermal fluids.

The chemical composition of steam vents was dominated by water (>99 mol%) followed by CO₂ (499-6,587 μmol/mol), H₂S (17.9-260.4 μmol/mol) and H₂ (10.2-194.2 μmol/mol). The composition of steam vents produced upon depressurization boiling of geothermal reservoir fluids differ within the region with steam vent gases being enriched in CO₂ and H₂S at Ölkelduháls relative to the Hveragerði region, those differences may be related to different heat source for both regions, Hrómundartindur volcanic systems on Ölkelduháls and Grændalur extinct volcanic system in Hveragerði. Gas geothermometry of steam vents estimate temperatures between 230-280°C in Hveragerði and 280-300°C in Ölkelduháls.

The surface manifestations were influenced by seismic events, the 2008 earthquake could either open and close fractures or faults rupture and affect the appearance of geothermal manifestations, especially alkaline hot springs reported on previous studies on Hveragerði town (boiled hot spring) and the vicinity of Varmá river that were not recognized during the 2020 survey; however, fumaroles keep the same characteristic in terms of CO₂, H₂S and H₂ concentration.

Útdráttur

Efnafræði jarðhitavatns og -gufu á yfirborði jarðhitasvæðanna í Hveragerði og á Ölkelduhálsi var rannsökuð. 43 vatns- og gufusýnum var safnað úr köldum lindum, ám, heitum laugum og gufuhverum, og efnasamsetning þeirra ákvörðuð.

Vatn úr heitum laugum hafði sýrustig á bilinu 6,06-8,69 og lágan styrk Cl (3,32-7,34 ppm), en SiO₂ (38,5-217 ppm) og CO₂ (6, 43-486 ppm) höfðu yfirleitt hæstan styrk uppleystra efna. Líkan var sett fram til að lýsa efnasamsetningu jarðhitavatns á yfirborði sem blöndu þriggja frumpátta, sem voru (1) soðinn djúpvökvi, (2) þétt gufa, og (3) kalt vatn. Þetta líkan gaf skýrt til kynna að vatnið í þeim laugum sem skoðaðar voru reyndist blanda af þéttri gufu og köldu vatni, í ólíkum hlutföllum. Ekkert laugasýnanna innihélt soðinn djúpvökva úr jarðhitakerfunum.

Gufa úr gufuhverum var að langtærstum hluta vatn (>99 mól-%) en aðrar helstu lofttegundir voru CO₂ (499-6587 µmól/mól), H₂S (17,9-260,4 µmól/mól) og H₂ (10,2-194,2 µmól/mól). Svæðisbundinn munur sést á efnasamsetningu gufunnar, og er gufa á Ölkelduhálsi greinilega ríkari að CO₂ og H₂S en gufa í Hveragerði. Þessi munur kann að tengjast því að hitagjafar jarðhitakerfanna eru ólíkir; Ölkelduháls tengist eldstöðvakerfi Hrómundartinds en Hveragerði kulnuðu eldstöðinni í Grændal. Efnahitamælar sem nota efnasamsetningu gufunnar, gáfu djúphitastig á bilinu 230-280°C í Hveragerði og 280-300°C á Ölkelduhálsi.

Yfirborðsvirkni á jarðhitasvæðunum breyttist nokkuð við jarðskjálftana árið 2008, enda getur jarðskjálftavirkni orðið til þess að sprungur opnast eða lokist, eða misgengi myndist, sem allt getur haft áhrif á ásýnd jarðhitavirkinnar. Sér í lagi fundust nú engir hverir með soðnu, basísku jarðhitavatni, en þá mátti áður finna í Hveragerði og við Varmá. Hins vegar virðist styrkur CO₂, H₂S og H₂ í gufu úr gufuaugum ekki hafa breyst.

Dedicated
to my beloved parents Mireya and Emilio, for their example and inspiration.

Table of Contents

Útdráttur	vi
List of Figures	xi
List of Tables.....	xiii
Acknowledgements	xv
1 Introduction.....	17
1.1 Geothermal activity in Iceland	17
1.2 Geothermal exploration.....	18
1.3 Study purpose	18
2 The study area.....	20
2.1 General Geology.....	20
2.2 Geothermal activity in the area based in previous studies	22
2.2.1 Ölkelduháls geothermal area.....	23
2.2.2 Hveragerði geothermal area	23
3 Methods.....	25
3.1 Sampling.....	25
3.2 Chemical analysis.....	27
3.3 Previous studies data	30
3.4 Data treatment	30
3.4.1 Reservoir fluid composition.....	30
3.4.2 Gas geothermometry	31
3.4.3 Quantification of fluid sources and mixing for hot springs	31
4 Results.....	33
4.1 Chemical composition of steam vent samples	33
4.2 Chemical composition of surface water samples	33
4.3 Chemical composition of boreholes fluids.....	36
5 Discussion	38
5.1 Reservoir fluid composition	38
5.2 Boiling, steam condensation and mixing process	38
5.3 Fluid- rock interaction	41
5.4 Geothermal steam vent discharges	44
5.4.1 Steam vent composition, boiling, condensation and gas separation.....	44
5.4.2 Gas geothermometry	46
5.5 Comparison with previous studies	47
5.6 Conceptual model.....	50
6 Conclusions.....	52

References	liii
Supplement 1: Chemical composition of steam vents from previous studies	lix
Supplement 2: Chemical comp. of thermal waters from previous studies	lxiii
Supplement 3: Reservoir fluid composition.....	lxvii
Supplement 4: Estimation of temperature with different gas geothermometers	68

List of Figures

Figure 1. Geology and geothermal activity in Iceland, High-temperature fields shown as red circles, and low-temperature areas are shown in dark circles (Steingrímsson, 2014).....	18
Figure 2. Geological map with its tectonic settings and volcanic system within the Hengill greater volcanic area (based on Árnason et al., 1986 and Sæmundsson et al., 2010).	21
Figure 3. Sampling survey: a) Field recognition in Gufudalur valley; b) Sampling of the steam vent GUF-38 in Gufudalur; c) Sampling of the carbonate spring ÖLK-03 in Ölkelduháls; d) Sampling of the hot spring GRÆ-27 in Grændalur.	27
Figure 4. Sampling points of the south side of Grændalur, Gufudalur and Hveragerði. Also shown are locations of previous studies sampling surveys.....	28
Figure 5. Water classification based on diagrams for: a) Temperature vs. chloride; b) sulphate vs. chloride; c) SO_4/Cl vs. pH and d) HCO_3 vs. chloride.....	40
Figure 6. Mixing ratios using the end-member composition: boiler reservoir water (brw), non-thermal waters (ntw) and condensed steam (cs) based on equations (12) to (14).....	41
Figure 7. Correlation plots of main constituents, a) chloride vs boron; b) chloride vs sodium; c) chloride vs iron; d) temperature vs sodium; e) temperature vs magnesium; b) temperature vs iron. For explanation of symbols see Figure 5	43
Figure 8. Spatial distribution of a) CO_2 and b) H_2S concentrations measured in steam vents.....	44
Figure 9. Relationship between H_2S and temperature; c) Relationship between SO_4 and temperature d) $H_2O-CO_2-H_2S$ gas ternary diagram; e) N_2-CO_2-Ar gas ternary diagram, b) N_2-H_2S-Ar gas ternary diagram.	45
Figure 10. a) N_2/Ar molar ratio – oxygen scatter plot; b) N_2/Ar molar ratio – nitrogen scatter plot. For legend symbol refers to Figure 9.	46
Figure 11. a) Scatter plot of temperatures based in H_2S geothermometer (Eq. 5) and CO_2 geothermometry (Eq. 3); b) Spatial distribution of gas geothermometry for 2020 survey. For symbol legend refers to Figure 9.....	47
Figure 12. a) Distribution of H_2S and CO_2 gases; b) H_2 and CO_2 gases en steam vents samples and comparsion with (Ívarsson et al., 2011b) research.....	48
Figure 13. Map of gas geothermometry changes after 2008 earthquake event and comparison of steam vents samples from preious studies (based on Ívarsson et al., 2011).....	49

Figure 14. Schematic conceptual model of the the study area (based in Geirsson & Arnórsson, 1995)..... 51

List of Tables

Table 1. Summary of previous studies on the geothermal area.....	22
Table 2. General information and geocoordinates of the sampling points.....	25
Table 3. Analytical methods, units, detection limits, standard solution and verification	29
Table 4. Gas geothermometry as a function of reservoir temperature	31
Table 5. The chemical composition of steam vent discharges. Concentrations are expressed in $\mu\text{mol/mol}$ total fluid.....	33
Table 6. Chemical components concentration of the water samples.....	34
Table 7. Borehole fluids composition reported in previous studies	36
Table 8. Composition of water end members, as measured or modeled. Units are in ppm	39

Acknowledgements

Sincere gratitude goes to the Government of Iceland through GRÓ Geothermal Training Programme (GRÓ-GTP) under the auspices of the United Nations Educational, Scientific and Cultural Organisation (UNESCO) for the financial support that made it possible to succeed in this project and this step on my professional career.

I would like to express my deepest gratitude to Ludvik Georgsson, ex-director of United Nations University – GTP (UNU-GTP) and Guðni Axelsson, current director of GRÓ-GTP for giving me the opportunity to start and continue the Master program in the University of Iceland. My studies took place during the transition period of UNU-GTP to GRÓ-GTP and the staff of the institution Ingimar, Vigdis, Málfríður, Markus continue giving me support and dedication throughout those two years. Many thanks for your dedicated job.

My appreciations to my supervisors Finnbogi Óskarsson and Andri Stefánsson for sharing their knowledge and experiences on the geothermal field. Their guidance, suggestions, and time teaching helped molding the ideas discussed in this report. The acknowledgements also go to ISOR Icelandic Geosurvey for hosting me during the sampling survey and chemical analysis and Orkuveita Reykjavíkur for the geothermal previous data on Ölkelduháls.

Special thanks to my friend Frida, her spontaneous help allowed to get over difficulties during the fieldwork. Despite sampling survey can become dangerous she kept giving her support to success this project.

Last but not less, to my geology friends, Tasnuva, Vivian, Diego, Erick, Vivi, Iciar, Patrick, Didas who helped me on the sampling survey. Besides learning sampling manifestations, we enjoyed the best places to perform a geochemical exploration.

1 Introduction

Geothermal activity in Iceland is widespread and relates to active volcanic systems and tectonics. Iceland is situated on the junction of the mid oceanic ridge (MOR) between the Eurasian and North-American plates and with the Icelandic mantle plume, making it a geologically active region. The Icelandic crust is characterized by a high heat flow, ~ 250 mW/m² within the rift zones and 90 mW/m² off-rift (Flóvenz and Sæmundsson, 1993). Within the rift zones, volcanic and geothermal activity is widespread whereas off-rift geothermal activity is often associated with active tectonics. Many of the geothermal fields have been explored for utilization with the geothermal resources being an important energy supply in Iceland and used for house heating, industry, greenhouses and electricity power production to name some. In 2019, the total direct use of geothermal energy in Iceland was estimated to be 9,328 GWh_{th} and the total installed electricity generation capacity from geothermal was 755 MW_e (Ragnarsson et al., 2021).

1.1 Geothermal activity in Iceland

The geothermal systems in Iceland have been divided into two groups, high- and low-temperature systems. High-temperature systems are mostly situated within the belt of active volcanism and rifting and characterized by thermal gradients of >150 - 200 °C/km and a magmatic heat source. Low-temperature geothermal systems are commonly associated in fractured rocks off-rift within the Quaternary and Tertiary formations and have thermal gradients of <150 °C/km (Bodvarsson, 1961; Fridleifsson, 1979). A general map of the geothermal areas in Iceland is shown in Figure 1.

Icelandic geothermal fluids are of meteoric and seawater origin or a mixture of them, with temperatures between ~ 10 and ~ 450 °C, pH of ~ 2 to ~ 10 and Cl concentrations of <1 to $>20,000$ ppm (Ármannsson, 2016; Kaasalainen et al., 2015; Kaasalainen & Stefánsson, 2012; Stefánsson, 2017). They have been divided into two groups: primary and secondary type fluids (Arnórsson et al., 2007). Primary fluids, sometimes referred to as reservoir fluids, are those reaching the deepest level within the geothermal system. With ascent to the surface, they can undergo chemical and physical changes leading to the formation of secondary geothermal fluids observed on surface, like hot springs, steam vents and mudpools.

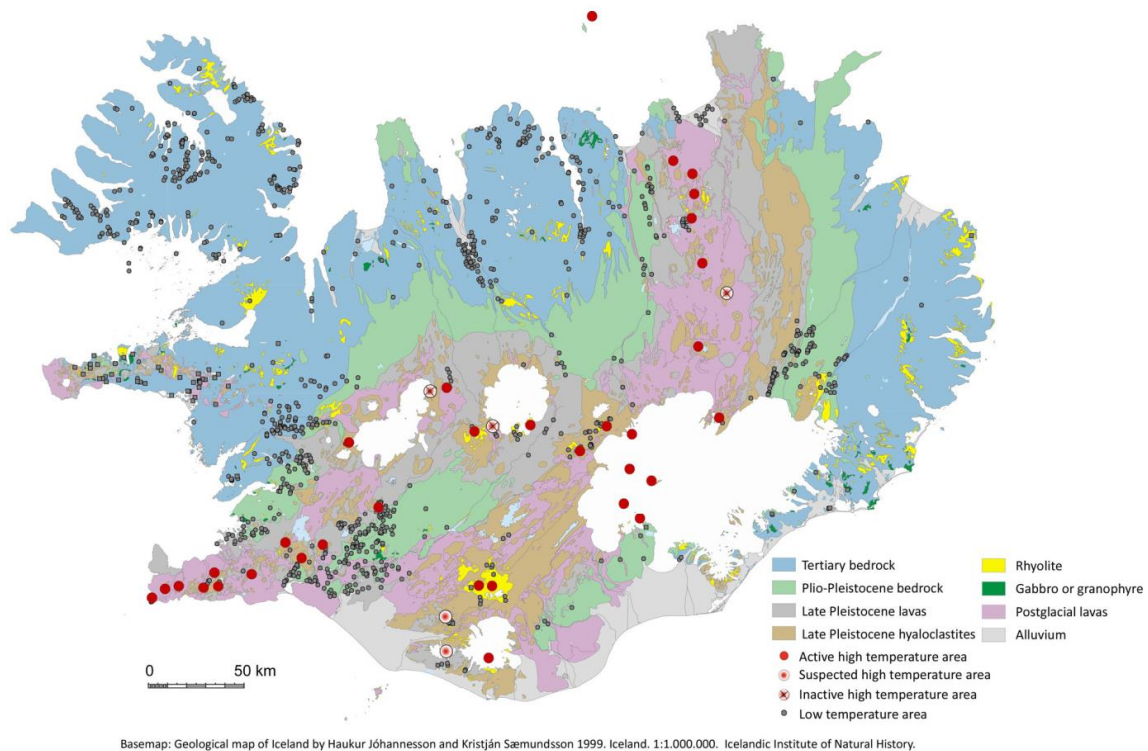


Figure 1. Geology and geothermal activity in Iceland, High-temperature fields shown as red circles, and low-temperature areas are shown in dark circles (Steingrímsson, 2014).

1.2 Geothermal exploration

The recognition of a geothermal resource involves geological, geochemical, and geophysical investigations with a reconnaissance and surface exploration study, followed by the assessment of all data available and the estimation of the size, reservoir temperature, energy potential etc. to construct a conceptual model of the system (Richter et al., 2010). A typical program for the exploration consists of: (1) preliminary study that also includes review of existing and available data; (2) geological study, with lithological mapping, structural geology, volcanism, hydrogeology; (3) geochemical survey, that includes fluid sample collection, analysis and interpretation; (4) geophysics surveys, with resistivity, gravimetry and magnetic methods to define the extension and dimension of the geothermal reservoir. The surface exploration often concludes with the definition of potential drilling targets that are part of the development plan (e.g., Steingrímsson, 2014).

1.3 Study purpose

The purpose of this study was to perform a geochemical survey of the Hveragerði and Ölkelduháls geothermal areas SW Iceland. Samples of surface geothermal fluids and non-thermal water were collected and analyzed, and the data interpreted using geochemical process models with the aim of constructing a geochemical conceptual model of the geothermal systems.

Questions of interest include:

- What are the chemical characteristics of geothermal fluids in the area and their spatial distribution?
- What are the processes affecting the composition of the geothermal fluids from source to surface?
- Have there been potential changes in the fluid geochemistry during past times and related to geological unrest in the area?

2 The study area

The study area includes three valleys and one ridge within the Hengill greater volcanic system, on the intersection of the Hrómundartindur and Grændalur volcanic systems. It is located 10 km north of Hveragerði town and 40 km southeast of Reykjavik. The landscape surrounding is peculiar, with geothermal manifestation throughout the three rivers. A geological map of the study area with its tectonic settings and volcanic systems is shown in Figure 2.

2.1 General Geology

The greater Hengill volcanic complex is located on a triple junction formed by the intersection of Reykjanes Peninsula (RVP), Western Volcanic Zone (WVZ) and South Iceland Seismic Zone (SISZ). It contains extensional structures related to three volcanic systems: Hengill, Hrómundartindur, and Grændalur; N-S strike-slip structures from the fissure swarms are characteristics of the transformation zone towards NE-SW spreading ridges as well as the area is entirely built up with quaternary and post-glacial volcanic events produced by an intensive tectonic activity through NE-SW volcanic fractures (Steigerwald et al., 2020).

The general geology is composed of hyaloclastites and interglacial lava flows related to the Upper Pleistocene and postglacial period, their composition is mostly basaltic ranging from picrite, olivine-tholeiitic to tholeiitic. These lavas and hyaloclastite form the base of the bedrock in the area (Kyagulanyi, 1996; Malik, 1996; Sæmundsson, 1979; Walker, 1992). Most of the fractures and faults are oriented NE-SW, NW-SE, and N-S; and, additionally, veins are filled by secondary minerals in areas of strong alteration caused by progressive burial. Petrographically, the rocks range from glassy tuffs, through holocrystalline tuffs to porphyritic tuffs (Eshetu Gemechu, 2017).

The main geothermal manifestations are located within active central volcanos or associated fissure swarms in the rift zone. The heat source for Ölkelduháls is considered to be magmatic intrusions in the upper crust, two NNE-WSSW striking volcanic fissures erupted in the Hengill volcano 2,000 and 5,500 years ago (Árnason et al., 1996; Mutonga, 2007). The Hrómundartindur volcanic system, which last erupted about 10 ka ago has experienced some more recent magma accumulation dates in 1994-1998 through earthquakes swarms (Clifton et al., 2002). On the other hand, The Grændalur zone, which is the oldest volcano system of the complex, presents pillow lavas and associated sediments of the upper Pleistocene about 0.7 Ma. Previous research proposed this system as the heat source of the Hveragerði geothermal area (Árnason et al., 1986; Mutonga, 2007).

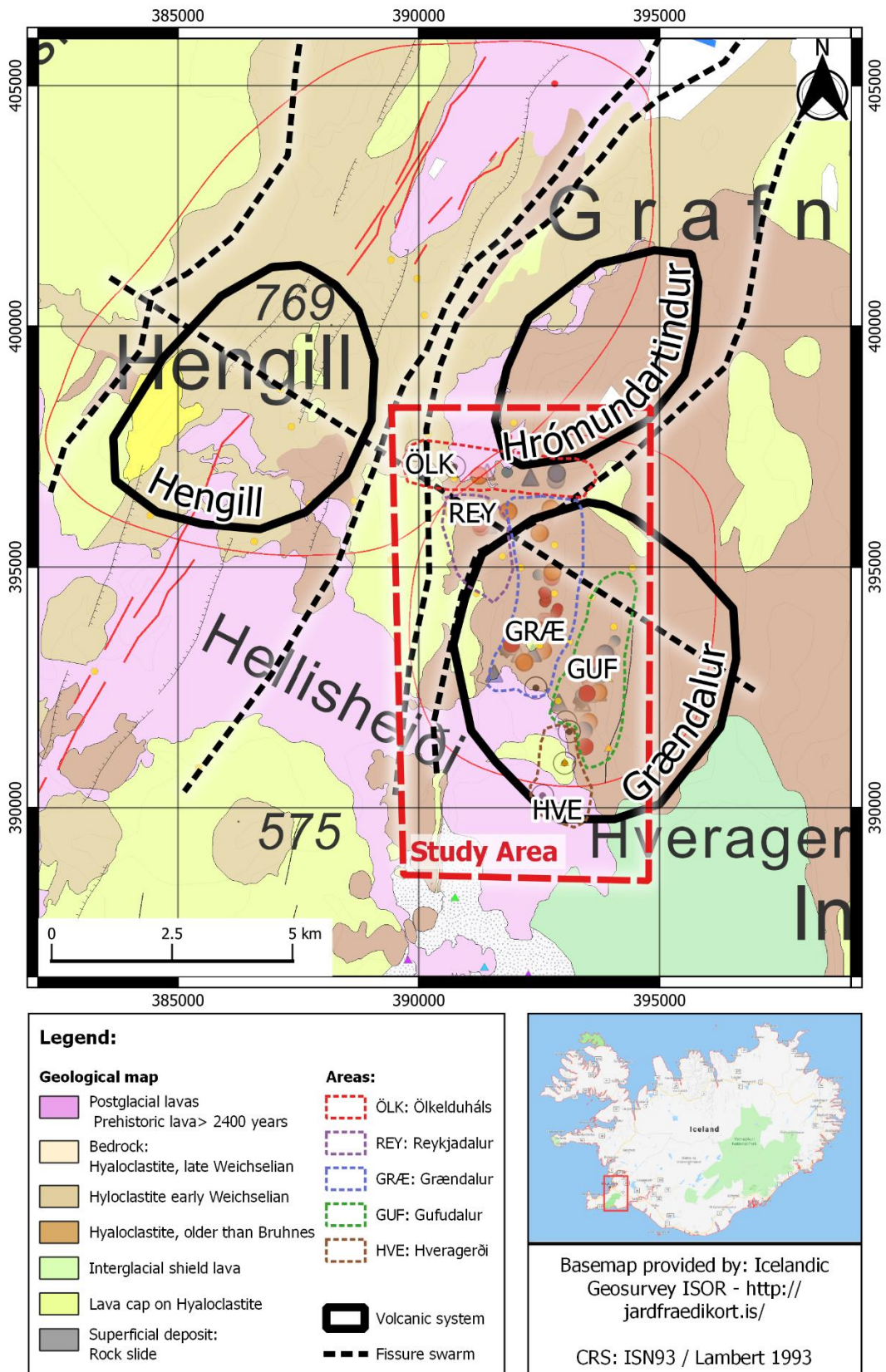


Figure 2. Geological map with its tectonic settings and volcanic system within the Hengill greater volcanic area (based on Árnason et al., 1986 and Sæmundsson et al., 2010).

2.2 Geothermal activity in the area based in previous studies

According to previous studies (Table 1), the study area encompasses two high-temperature geothermal fields, Ölkelduháls and Hveragerði, that are associated with two volcanic systems, Hrómundartindur in the northwest and Grændalur in the southeast (Figure 2). The Ölkelduháls system has been described as a carbon dioxide rich system originating from magmatic CO₂ with measured temperature in geothermal wells up to 280°C. The Hveragerði field has been described as a geothermal system in its final stage of a cooling process with seawater component in the reservoir and condensation separation process in the upflow steam vents. (Björnsson, 2007; Geirsson & Arnórsson, 1995).

Table 1. Summary of previous studies on the geothermal area

Research	Description
Xi-Xiang, 1980	Interpretation of 8 boreholes in the Ölfusdalur area including Hveragerði, it defined measured temperature, temperature gradient and aquifer deep.
Arnórsson & Gunnlaugsson, 1985	Gas geothermometry of fifteen steam vents on the vicinity of Hveragerði and the drillholes, wellhead temperatures decrease from 230°C in the north part to 160°C in the south. Discrepancy on CO ₂ and H ₂ S, H ₂ and CO ₂ -H ₂ geothermometry were observed due to the condensation / phase separation process in the upflow steam vents.
Gestsdóttir & Geirsson, 1990	Subsurface temperature estimation between 240-250°C obtained by water and gas geothermometry and the chemical composition of hot springs, steam vents, and well discharges.
Arnórsson & Andrésdóttir, 1995	Distribution of conservative components in water, defining the Cl/B ratio in water and discharged wells through Hveragerði area, the high Cl concentration was explained by a seawater component in the groundwater system.
Geirsson & Arnórsson, 1995	Conceptual model of Hveragerði geothermal field, with reservoir temperatures of 240-250°C, mixing between seawater and meteoric water in the reservoir.
Ívarsson, 1998	Estimation of subsurface temperature based in gas geothermometry for Hengill area including Ölkelduháls, suggesting that Ölkelduháls and Nesjavellir geothermal areas are not connected.
Zhanxue & Linchuan, 1998	Solute geothermometry with reservoir temperatures of 183-204°C and gas geothermometry temperatures of 210-260°C in Hveragerði area.
Björnsson, 2007	Conceptual model of Hengill geothermal areas included Ölkelduháls based on geothermal well data, with reservoir temperature of 210-280°C.
Ívarsson et al., 2011	Reconnaissance of geothermal manifestation in Reykjadalur, Grændalur and Gufudalur valleys with an interest in gas geothermometry to estimated subsurface temperature and thermic power.

Kaasalainen & Stefánsson, 2011	Speciation of aqueous dissolved sulfur in hydrothermal waters including Hveragerði controlled by the kinetics and the total sulfur source.
Kaasalainen & Stefánsson, 2012	Geochemistry of trace elements in surface water and steam including the Hveragerði geothermal field.
Khodayar & Björnsson, 2014	Analysis of surface ruptures and geothermal manifestations along the new fissures caused by the 2008 earthquake event. A fault ruptured over 20 km length at depth.
Kaasalainen et al., 2017	Geochemistry of Fe(II) and Fe(III) in natural geothermal waters including Ölkelduháls ridge influenced by the water pH that reflects the water type and the various processes resulting in their formation.
Eshetu Gemechu, 2017	Reconnaissance of geothermal manifestation in Grændalur valley to examine the relationship with geological structures and the changes occurred after the 2008 earthquake event.
Stefánsson, 2017	Geochemical composition of geothermal gases in Iceland including Hveragerði

2.2.1 Ölkelduháls geothermal area

Ölkelduháls is a ridge in the north part of the study area. The geothermal field lies within Hrómundartindur and Grændalur volcanic systems (Gudmundsson & Brandsdóttir, 2010). The topography of Ölkelduháls involves volcanic hills and NE-SW trending ridges with the highest peaks in the area about 800 m a.s.l. while ridge elevations are between 280 and 460 m a.s.l. The geothermal activity is controlled by tectonic features and transforms fault zone with an NW-SE trend through the manifestation from west to east (Okedi, 2006).

The geothermal activity in the area includes steam vents, boiling mud pools, hot springs, steaming grounds and extensive area of surface alteration. Two rivers, Grændalsá and Reykjadalsá, derived from both cold and hot springs, drain the area towards the south and west (Natukunda, 2005). Geothermal reservoir fluid temperatures based on gas geothermometry indicate subsurface temperatures above 300°C (Ívarsson, 1998). Three wells have been drilled on the area, they present extremely permeable formation at 1000-1200°C with highest measured temperature of 256°C on HE-20 geothermal well (Björnsson, 2007)

2.2.2 Hveragerði geothermal area

Hveragerði geothermal area includes the Hveragerði town located about 50 km east of Reykjavik and its surroundings that present geothermal manifestations. Within the area, there are 17 geothermal wells; 8 wells are labeled HV and 9 labeled HS. Some of the geothermal wells provide energy to the heating system, hot water and services to the town (Bragadóttir, 2019). The Hveragerði geothermal field is commonly divided into four sub-areas and include the valleys Reykjadalur, Grændalur and Gufudalur as well as the town Hveragerði and its surroundings.

Reykjadalur is a valley south of Ölkelduháls. The area is well known as a tourist attraction due to the hot river Reykjadalsá which has a comfortable bathing temperature year around. The geothermal activity in Reykjadalur is characterized by steaming ground and hot springs that feed the river running down the valley.

East of Reykjadalur lies Grændalur, followed by Gufudalur. Grændalur is separated from the other valleys by agglomerate basalt units, Dalafell on the west and Tindar in the east. Those hyaloclastites are the topographic boundary of the valleys but landslide deposits cover the area within the depression (Kyagulanyi, 1996). The river Grændalsá comes from the Álfatjörn lake, flows through the Grændalur valley and is then joined with Reykjadalsá. The resulting river is from then on called Varmá. Geothermal manifestations in Grændalur and Gufudalur are somewhat similar, characterized by steam vents and hot spring, thermal rivers and streams and mud pools.

Hveragerði field is situated south of the three valleys within and around the Hveragerði town. The geothermal activity in Hveragerði is characterized by hot springs, steam vents and mud pools, the water classification based on cations and anions diagram showed Na-HCO₃ and NaCl waters. The water manifestations mainly corresponded to steam heated waters and boiled waters recognized in the conceptual model using carbonate-silica mixing models (Geirsson & Arnórsson, 1995) 17 geothermal wells were drilled for commercial and scientific purposes, the geothermal wells are located within this part of the area where the measured temperature goes from 215°C to 230°C on the northern part, and from 167°C to 198°C for the southern part. The conceptual model for the area estimates a maximum reservoir fluid temperature about 250°C (Geirsson & Arnórsson, 1995).

3 Methods

3.1 Sampling

Sampling of surface geothermal fluids was carried out between 23 September and 14 November 2020 (Figure 3). In total, 43 samples were collected that included 7 river samples, 6 cold springs, 15 hot springs, and 15 steam vents. Sample locations are listed in Table 2 and shown in Figure 4.

Water samples were collected using previously described methods (Arnórsson et al., 2006; Ármannsson & Ólafsson, 2007). Four sample aliquots were collected at each site. For determination of pH, CO₂ and conductivity an untreated sample was collected to a 250 mL amber-glass bottle. For determination of major cations, the samples were filtered (0.2 µm cellulose acetate) into 100 mL HDPE bottles and acidified using concentrated HNO₃ acid (Suprapur Merck, 1 mL acid to 100 mL sample). Samples for determination of major anions were also filtered (0.2 µm cellulose acetate) into 100 mL HDPE bottles but not further treated.

Steam vents samples were collected into evacuated and pre-weighed 250 mL gas bulbs that contained ~50 mL of 40% NaOH. For sampling, a funnel was placed over the steam outflow and covered with soil to prevent atmospheric air contamination. The funnel was connected to a titanium tube and reaches the gas bulb via silicone tubing. A piece of tubing, about 5 cm in length, is connected to the distal sample port and fitted with a clamp, after flushing the sample ports with steam for about 2 min, the clamp is closed, and the bottle is opened to collect the sample while cooling continuously (Arnórsson et al., 2006).

Table 2. General information and geocoordinates of the sampling points

Sample	Label	Sampling date	Type	North ISN93	West ISN93	Altitude [m]
YF20-001	ÖLK-01	23.09.2020	River	396866	392318	352
YF20-002	ÖLK-02	23.09.2020	Cold spring	396810	392848	347
YF20-003	ÖLK-03	23.09.2020	Cold spring	396942	392865	360
YF20-004	ÖLK-04	23.09.2020	Steam vent	396898	391254	393
YF20-005	REY-05	23.09.2020	Hot spring	395920	391165	277
YF20-006	REY-06	23.09.2020	Hot spring	395875	391377	272
YF20-007	REY-07	23.09.2020	River	395877	391446	273
YF20-008	REY-08	23.09.2020	Hot spring	395812	391286	287
YF20-009	REY-09	24.09.2020	Steam vent	395958	392605	240
YF20-010	GRÆ-10	24.09.2020	Hot spring	396016	392592	233
YF20-011	GRÆ-11	24.09.2020	Steam vent	396154	391858	367
YF20-012	REY-12	24.09.2020	Hot spring	395891	391264	273
YF20-013	REY-13	24.09.2020	Steam vent	396070	391108	287
YF20-014	REY-14	24.09.2020	River	396164	391106	281
YF20-015	REY-15	24.09.2020	Steam vent	396197	390700	347
YF20-016	GRÆ-16	15.10.2020	Hot spring	395702	392533	232
YF20-017	GRÆ-17	15.10.2020	Hot spring	394781	392760	204

YF20-018	GRÆ-18	16.10.2020	Steam vent	396209	392739	274
YF20-019	GRÆ-19	16.10.2020	Steam vent	395702	392508	239
YF20-020	GRÆ-20	16.10.2020	Steam vent	394897	392776	210
YF20-021	GRÆ-21	16.10.2020	Steam vent	393265	392574	212
YF20-022	GRÆ-22	20.10.2020	Hot spring	393796	392608	131
YF20-023	GRÆ-23	20.10.2020	Hot spring	393706	392513	140
YF20-024	GRÆ-24	20.10.2020	River	393215	392370	84
YF20-025	GRÆ-25	20.10.2020	Steam vent	393681	392490	144
YF20-026	GRÆ-26	20.10.2020	Steam vent	393018	392190	80
YF20-027	GRÆ-27	20.10.2020	Hot spring	393399	391924	107
YF20-028	GRÆ-28	20.10.2020	River	392789	391567	91
YF20-030	GUF-30	03.11.2020	Steam vent	393180	393819	183
YF20-031	GUF-31	03.11.2020	Cold spring	393186	393831	184
YF20-032	GUF-32	03.11.2020	Cold spring	393195	393868	195
YF20-033	GUF-33	03.11.2020	Hot spring	392983	393708	162
YF20-034	GUF-34	03.11.2020	Hot spring	392930	393714	174
YF20-035	GUF-35	03.11.2020	Cold spring	392756	393748	177
YF20-036	GUF-36	03.11.2020	Steam vent	392393	393725	232
YF20-037	GUF-37	10.11.2020	Hot spring	392371	393496	118
YF20-038	GUF-38	10.11.2020	Steam vent	391776	393524	142
YF20-039	GUF-39	10.11.2020	Hot spring	391602	393322	80
YF20-040	GUF-40	10.11.2020	Cold spring	391598	393421	96
YF20-041	GUF-41	10.11.2020	Steam vent	391266	393414	71
YF20-042	GUF-42	10.11.2020	Hot spring	391267	393455	75
YF20-043	GUF-43	10.11.2020	River	391789	393007	60
YF20-044	GUF-44	14.11.2020	River	392186	392907	67





Figure 3. Sampling survey: a) Field recognition in Gufudalur valley; b) Sampling of the steam vent GUF-38 in Gufudalur; c) Sampling of the carbonate spring ÖLK-03 in Ölkelduháls; d) Sampling of the hot spring GRÆ-27 in Grændalur.

3.2 Chemical analysis

The chemical analysis of water composition involved both on-site and laboratory analysis. A summary of the analytical methods and related information are summarized in Table 3. On-site, the concentration of dissolved H_2S was analyzed using a Hg-precipitation titration and the pH determined using a combination glass electrode. In the laboratory, the major anions (F, Br, Cl, SO_4) were analyzed using ion chromatography (Dionex ICS-2100). The concentration of major cations (SiO_2 , B, Na, K, Ca, Mg, Al, Fe) and selected trace elements (As, Ba, Cr, Cu, Mo, Li, Mn, Mo, Ni, Zn, Ti) were analyzed using Inductively coupled plasma - optical emission spectrometry (ThermoScientific iCAP 7400 ICP-OES). Dissolved inorganic carbon (CO_2) and electrical conductivity were analyzed within two days after sampling using a modified alkalinity titration and conductivity meter, respectively.

The concentration of CO_2 and H_2S in steam vent samples were analyzed in the steam condensate using the previously mentioned titrimetric methods for H_2S and CO_2 . Non-condensable gases (CH_4 , H_2 , N_2 , O_2 , and Ar) were further analyzed using a gas chromatography (GC, Perkin Elmer Arnel GC PEA-4019) with thermal conductivity detectors. The amount of water was determined gravimetrically.

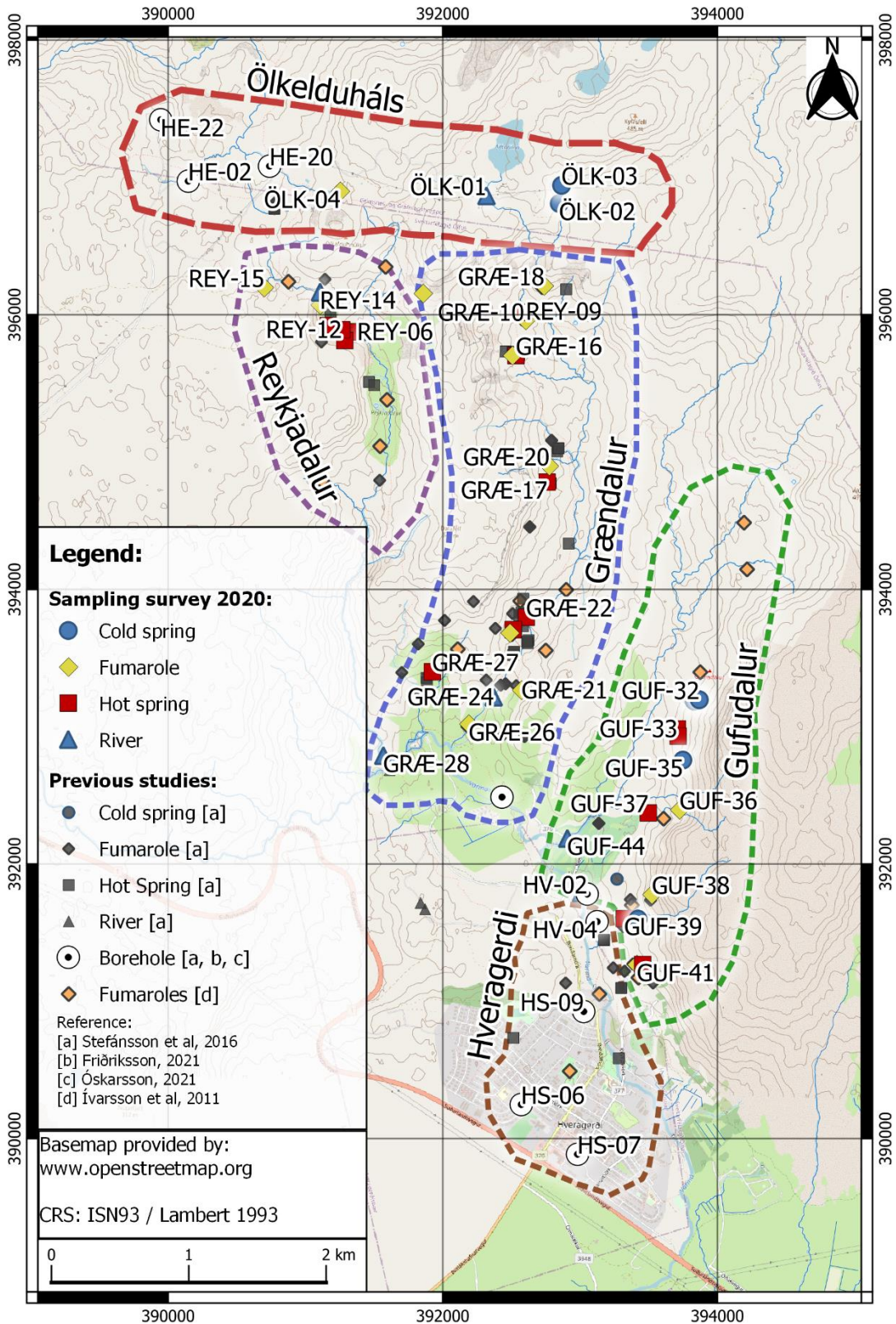


Figure 4. Sampling points of the south side of Grændalur, Gufudalur and Hveragerði. Also shown are locations of previous studies sampling surveys.

Table 3. Analytical methods, units, detection limits, standard solution and verification

Component	Analytical Method	Measurement Concentration range (ppm)	Detection Limit (ppm)	Analytical standards used	Verification method	
<i>Liquid phase</i>	CO ₂	Titration	< 20	-	Triplicate analysis	
	H ₂ S	On-site titration	0.01 - 0.3	0.01	Duplicate analysis	
	F	IC	0.01 - 2.00	0.01	Standard solution (a)	Triplicate analysis and measurement comparison (e)
	Cl	IC	0.01 - 100.00	0.01		
	Br	IC	0.01 - 20.00	0.01		
	SO ₄	IC	0.01 - 100.00	0.01		
	Al	ICP-OES	0.005 - 1.00	0.005		
	As, B	ICP-OES	0.003 - 2.00	0.003	Standard solution (b)	Triplicate analysis and measurement comparison (e)
	Ba	ICP-OES	0.0002 - 2.00	0.0002		
	Ca	ICP-OES	0.004 - 50.00	0.004		
	Cr, Cu	ICP-OES	0.002 - 1.00	0.002		
	Mo	ICP-OES	0.001 - 1.00	0.001		
	K	ICP-OES	0.2 - 10.00	0.2		
	Li	ICP-OES	0.008 - 1.00	0.008		
	Mg	ICP-OES	0.01 - 1.00	0.01		
	Mn	ICP-OES	0.0003 - 1.00	0.0003		
	Mo	ICP-OES	0.002 - 1.00	0.002		
	Na	ICP-OES	0.04 - 100.00	0.04		
	Ni	ICP-OES	0.0003 - 1.00	0.0003		
	Zn	ICP-OES	0.0002 - 1.00	0.0002		
Sr.	ICP-OES	0.1 - 4.00	0.0005			
Ti	ICP-OES	0.002 - 1.00	0.002			
SiO ₂	ICP-OES	0.12 - 50.00	0.12			
<i>Gas-phase</i>	CO ₂ and H ₂ S	Titration			Triplicate analysis	
	H ₂	GC - LGA		0.01 %-vol	Gas mixture (c)	measurement comparison (c, d)
	CH ₄	GC - LGA		0.01 %-vol		
	O ₂	GC - Ar		0.01 %-vol	Gas mixture (d)	
	N ₂	GC - Ar		0.01 %-vol		
	Ar	GC - Ar		0.01 %-vol		

(a): Seven calibration solutions prepared from the dilution of 1000 mg/L primary standard solution (Merck TraceCERT) for all four ions.

(b): Five calibration solutions prepared from the dilution of a 1000 mg/L primary standard solution (Merck TraceCERT) for all analysis cations and trace elements.

(c): Measured using a certified standard from Linde gas with known concentrations for each gas. The gas standard contains 19.8% H₂, 30.0% CO₂ and 10.0% CH₄.

(d): Measured using atmospheric air as standard. Concentrations 78.1% N₂, 21.0% O₂ and 0.93% Ar.

(e): Measured comparison every 5-7 samples with a reference sample that can be: VMS-G (in-house reference sample), Kalt Ru (in-house reference sample), Dionex CRM with 5 anions at known concentrations (F, Cl, NO₃, PO₄, SO₄), or Permixon (Merck TraceCERT-CRM with 33 elements at known concentrations). Silica is determined against the Spóastaðir in-house standard.

For the water analysis, the precision is expressed in terms of: (1) Relative standard deviations (RSD) between the triplicate analysis. Their values range would depend on the instrument, parameter, and sample analyzed. In general, for the total set of analysis: the ICP analysis below 3.5%, for IC analysis below 4.8%, for titration below 3% and no data of GS (2) Recovery percent between the standard analysis measurement comparison, those include the comparison of the reported standard concentration with the obtained measurement during the analysis. The recovery percent ICP analysis is an average of 94 – 108%, compared to Permixon standard; IC analysis is an average of 95-110%, compared to VMS-G standard.

3.3 Previous studies data

The current dataset was extended using previously published values of surface geothermal and borehole fluids. These included 28 samples of cold springs, hot springs and acid hot springs, 56 steam vents and 6 boreholes sampled from 1982 to 2019 (Arnórsson & Andréðóttir, 1995; Arnórsson & Gunnlaugsson, 1985; Ívarsson et al., 2011a; Kaasalainen & Stefánsson, 2012; Stefánsson, 2017, Óskarsson, 2020).

Chemical analysis of three boreholes from Ölkelduháls were obtained from Orkuveita Reykjavíkur (Friðriksson, personal communication, March 4, 2021).

3.4 Data treatment

The geochemical treatment of the data included: calculation of reservoir fluid composition from data based on well fluid discharges previously published, assessment of source and mixing of surface geothermal water and gas geothermometry.

3.4.1 Reservoir fluid composition

The calculations of reservoir fluid composition from data for two-phase (liquid and steam) borehole fluid composition were carried out using the WATCH program, version 2.4 (Bjarnason, 2010). For these calculations, liquid only reservoir fluids were assumed and adiabatic boiling from reservoir to surface. The calculations of the reservoir fluid composition are based thus on conservation of enthalpy and mass,

$$m_i^{f,t} = m_i^{d,t} = X^{d,v}m_i^{d,t} + (1 - X^{d,v})m_i^{d,lq} \quad (1)$$

$$h^{f,t} = h^{d,t} = X^{d,v}h^{d,v} + (1 - X^{d,v})h^{d,lq} \quad (2)$$

where m_i denotes the molal concentration of the i -th component, X is the vapor fraction, h is the enthalpy, and f , t , d , v , and lq are the fluid, total, discharge, vapor, and liquid phase, respectively.

3.4.2 Gas geothermometry

Gas geothermometry was calculated using previously published temperature functions as shown in Table 4 (Arnórsson & Gunnlaugsson, 1985). Nine different equations (Equation 3 to 11) were applied, that are based on gas-mineral and gas-gas equilibria. In some cases, possible steam condensation occurring upon fluid ascent to surface are considered for these gas geothermometers.

Table 4. Gas geothermometry as a function of reservoir temperature

Geothermometer	Temperature function	Equation
[CO ₂]	$T = -44.1 + 269.25 \cdot Q - 76.88 \cdot Q^2 + 9.52 \cdot Q^3$	(3)
[F - T]	$T = 244.6 - 17.447 \cdot Q - 0.16 \cdot Q^2 - 0.0524 \cdot Q^3$	(4)
[H ₂ S]	$T = 246.7 + 44.81 \cdot Q$	(5)
[H ₂]	$T = 277.2 + 20.99 \cdot Q$	(6)
[CO ₂ /H ₂]	$T = 341.7 - 28.57 \cdot Q$	(7)
[H ₂ S/H ₂]	$T = 304.1 - 39.48 \cdot Q$	(8)
[H ₂ S]	$T = 173.2 + 65.04 \cdot Q$	(9)
[H ₂]	$T = 212.2 + 38.59 \cdot Q$	(10)
[CO ₂ /H ₂]	$T = 311.7 - 66.72 \cdot Q$	(11)

Equations 3 and 4 use temperature as a function of CO₂ concentration and the equilibrium constant for the Fischer–Tropsch reaction that involves CO₂, CH₄, and H₂ concentrations in steam vent steam. Equations 5, 6, 7, 8 use concentration of H₂S, H₂, CO₂/H₂ and H₂S/H₂ respectively, those are adjusted to either all water reservoir temperature above 300°C or water reservoir in the range 200-300°C with chloride concentration over 500 ppm. Equations 9, 10, and 11 use concentrations of H₂S, H₂, and CO₂/H₂ respectively and are adjusted to either all water reservoirs below 200°C or water reservoir in the range 200-300°C with chloride concentration below 500 ppm.

3.4.3 Quantification of fluid sources and mixing for hot springs

In a geothermal system, thermal fluids ascend from the reservoir to the surface due to density driven circulation through fractures or up-flow zones. During such ascent, several processes may affect the water composition, including boiling and formation of steam and boiled liquid water and mixing with non-thermal surface and shallow ground water (Arnórsson et al., 2007).

Following Stefánsson et al., (2016b) the end-member producing various geothermal fluid features at surface may include: (1) boiled reservoir water (brw), (2) non-thermal waters(ntw) and (3) condensed steam (cs) and mixtures thereof. Assuming Cl and temperature to be preserved upon mixing of the various end-member components, the system can be described by three equations:

$$m_{Cl}^m = X^{cs} m_{Cl}^{cs} + X^{brw} m_{Cl}^{brw} + X^{ntw} m_{Cl}^{ntw} \quad (12)$$

$$T_{Cl}^m = X^{cs} T_{Cl}^{cs} + X^{brw} T_{Cl}^{brw} + X^{ntw} T_{Cl}^{ntw} \quad (13)$$

$$1 = X^{cs} + X^{brw} + X^{ntw} \quad (14)$$

where X is the fraction of each endmember, T is temperature in °C, m_{Cl} is the chloride concentration in ppm.

To solve for X^{cs} , X^{brw} and X^{ntw} we apply Cramer's rule to obtain,

$$X^{cs} = D^{cs}/D \quad (15)$$

$$X^{brw} = D^{brw}/D \quad (16)$$

$$X^{ntw} = D^{ntw}/D \quad (17)$$

where,

$$D = m_{Cl}^{cs}(T^{brw} - T^{ntw}) - T^{cs}(m_{Cl}^{brw} - m_{Cl}^{ntw}) + (m_{Cl}^{brw} T^{ntw} - m_{Cl}^{ntw} T^{brw}) \quad (18)$$

$$D^{cs} = m_{Cl}^m(T^{brw} - T^{ntw}) - T^m(m_{Cl}^{brw} - m_{Cl}^{ntw}) + (m_{Cl}^{brw} T^{ntw} - m_{Cl}^{ntw} T^{brw}) \quad (19)$$

$$D^{brw} = m_{Cl}^{cs}(T^m - T^{ntw}) - T^{cs}(m_{Cl}^m - m_{Cl}^{ntw}) + (m_{Cl}^m T^{ntw} - m_{Cl}^{ntw} T^m) \quad (20)$$

$$D^{ntw} = m_{Cl}^{cs}(T^{brw} - T^m) - T^{cs}(m_{Cl}^{brw} - m_{Cl}^m) + (m_{Cl}^{brw} T^m - m_{Cl}^m T^{brw}) \quad (21)$$

With this approach negative values are possible as well as values greater than 1. Such values have no physical relevance as the source of a given end-member water cannot be <0% and >100%. The physical reason for such negative values is thought to be temperature decrease due to conductive cooling to the surroundings, loss of water mass through evaporation, natural variability of the end-member fluid composition and/or uncertainties associated with the chemical analysis of individual water samples (Stefánsson et al., 2016b).

The end-member fluid types composition can be assessed through WATCH program (Bjarnason, 2010) assuming adiabatic boiling from the reservoir condition to the surface at 100°C. Two phases wellhead discharged from previous studies datasets (Supplement 3) were modeled to estimate water end member composition:

- (1) Geothermal reservoir waters (gr), based on the species composition of the reconstruction of the reservoir.
- (2) Boiled reservoir waters (brw) were estimated based on the adiabatic boiling of the geothermal reservoir upon surface at 100°C and 1 bar.
- (3) Condensed steam (cs) were obtained under the same model of boiled geothermal reservoir using the steam phase at 100°C and 1 bar and followed by the aqueous speciation with PHREEQC.
- (4) Non-thermal waters (ntw), represented by the average of rivers and cold spring on the area with an average of 7 ppm of chloride and temperature below 9°C.

4 Results

4.1 Chemical composition of steam vent samples

In total, 14 steam vent samples were collected and analyzed for H₂O, CO₂, H₂S, H₂, CH₄, N₂, O₂, and Ar (Table 5). In addition, 56 steam vents samples previously reported were compared with the data obtained in the study (Supplement 1).

The steam vent fluids are dominated by water vapor for both Ölkelduháls and Hveragerði geothermal fields with accounting for 98.9-99.9 mol%. The steam vent fluids are generally more gas rich at Ölkelduháls with CO₂, H₂S and H₂ concentrations of 4944-9984 µmol/mol, 195-389 µmol/mol and 97-213 µmol/mol compared to at Hveragerði 499-7812 µmol/mol, 12-260 µmol/mol and 1-247 µmol/mol, respectively. The concentrations of other gases for non-air contaminated samples were generally low.

Table 5. The chemical composition of steam vent discharges. Concentrations are expressed in µmol/mol total fluid.

Sample	Label ^(a)	Temp. [°C]	H ₂ O	CO ₂	H ₂ S	H ₂	CH ₄	O ₂	N ₂	Ar
YF20-004	ÖLK-04	97.3	993061	6587	195	149	4.46	0.37	3.2	0.04
YF20-009	REY-09	98.3	998008	1814	96.0	52.3	1.67	2.17	25.3	0.34
YF20-011	GRÆ-11	98.4	997321	2393	166	92.7	1.08	0.02	26.0	0.39
YF20-013	REY-13	98.5	997710	2124	105	54.7	0.85	nd	5.2	0.10
YF20-015	REY-15	91.7	995740	3910	249	90.8	2.12	nd	7.7	0.17
YF20-018	GRÆ-18	98.2	997722	2132	93.4	30.3	1.57	nd	20.3	0.37
YF20-019	GRÆ-19	97.4	997562	2157	211	52.5	1.37	nd	16.0	0.30
YF20-020	GRÆ-20	96.3	997854	1928	115	34.3	1.87	0.01	64.8	1.34
YF20-021	GRÆ-21	97.5	998221	1541	116	86.8	1.50	1.61	31.2	0.54
YF20-025	GRÆ-25	98.8	997112	2331	260.	194	3.95	nd	96.8	1.81
YF20-030	GUF-30	97.8	998604	1169	60.2	48.7	4.40	0.06	110	2.35
YF20-036	GUF-36	98.1	997838	1994	58.0	45.0	2.77	0.01	60.8	1.29
YF20-038	GUF-38	98.2	999203	736	32.4	10.2	0.48	nd	16.8	0.35
YF20-041	GUF-41	93.8	999429	499	17.9	10.3	0.51	0.28	42.6	nd

(a): The suffix label refers to the sampling area as: ÖLK: Ölkelduháls, REY: Reykjadalir, GRÆ: Grændalur, GUF: Gufudalur.

4.2 Chemical composition of surface water samples

In total, 28 samples of surface waters were collected, including cold and geothermal springs and rivers. The results are reported in Tables 6. In addition, previous results on surface water composition were gathered (Supplement 2).

Table 6. Chemical components concentration of the water samples

Sample	Label	Temp [°C]	pH / Temp	Cond [mΩ]	CO ₂ [ppm]	H ₂ S [ppm]	F ⁻ [ppm]	Cl ⁻ [ppm]	Br ⁻ [ppm]	SO ₄ ²⁻ [ppm]	Al [ppm]	B [ppm]	Ba [ppm]	Ca [ppm]
YF20-001	ÖLK-01	3.6	7.74	0.087	23.9	0	0.034	6.26	0.012	4.27	0.005	0.002	0	5.85
YF20-002	ÖLK-02	5.2	7.91	0.095	18.6	0	0.053	7.57	0.015	13.3	0.001	0.003	<0.001	7.34
YF20-003	ÖLK-03	12	5.45	0.346	844	0.08	0.098	5.94	0.029	7.07	0.106	0.074	0.006	23
YF20-005	REY-05	80.4	6.25 / 19.5°C	0.478	414	0	0.239	6.74	0.017	23.7	0.005	0.003	0.039	61.6
YF20-006	REY-06	35	6.7 / 30°C	0.345	174	0.04	0.169	6.55	0.015	15.6	0.007	0.002	0.015	31.8
YF20-007	REY-07	7.9	8.38	0.077	47.5	0	0.053	5.56	0.013	16.2	0.01	0.002	0.001	14.7
YF20-008	REY-08	25.3	7.84	0.362	240	0	0.263	7.34	0.015	13.3	0.009	0.009	0.002	32.4
YF20-010	GRÆ-10	77	7.24 / 27°C	0.315	140	0	0.006	5.2	0.024	14.5	0.036	0	<0.001	27.2
YF20-012	REY-12	79.5	6.87 / 25°C	0.632	486	0	0.231	6.6	0.017	25	0.005	0.003	0.044	65.7
YF20-014	REY-14	7.8	8.33	0.11	21.8	0	0.016	6.03	0.013	15.3	0.019	0	0.001	8.6
YF20-016	GRÆ-16	92	7.21 / 24°C	0.153	20.2	0.14	0.016	6.03	0.013	15.3	0.141	0	0.003	17.3
YF20-017	GRÆ-17	90	6.06 / 22°C	0.216	12.6	0.15	0.033	5.51	0.015	39.2	0.096	0	0.003	18.4
YF20-022	GRÆ-22	96	8.69 / 30°C	0.287	57.9	0	0.319	6.08	0.018	48.6	0.196	0.009	0.002	2.26
YF20-023	GRÆ-23	75.5	8.15 / 22°C	0.255	40.7	0	0.334	6.61	0.036	54	0.085	0.005	0.049	7.8
YF20-024	GRÆ-24	8	7.85	0.244	79.3	0	0.053	5.74	0.02	20.7	0.011	0.004	0.003	27.1
YF20-027	GRÆ-27	42	7.32 / 25°C	0.345	131	0	0.051	6.83	0.02	26.2	0.007	0.006	0.001	28.9
YF20-028	GRÆ-28	9.2	8.15	0.251	87.7	0	0.094	6.67	0.016	15.6	0.008	0.003	0.005	23.3
YF20-031	GUF-31	5.7	7.61	0.139	38.7	0	0.062	6.02	0.012	14.3	0.006	0.003	0	12.6
YF20-032	GUF-32	2.2	8.04	0.133	38.4	0	0.064	6.03	0.011	13.4	0.006	0.002	<0.001	12.5
YF20-033	GUF-33	93.3	8.58 / 20.4°C	0.127	23.8	0.1	0.013	3.32	0.013	22	0.066	0.007	0.002	3.78
YF20-034	GUF-34	78.4	6.66 / 38.3°C	0.378	82	0.11	0.012	6.01	0.02	111	0.008	0.004	0.016	52.4
YF20-035	GUF-35	10.5	7.31	0.24	104	0	0.046	7.16	0.017	5.65	0.002	0.002	0.001	31.7
YF20-037	GUF-37	76.7	6.9 / 22°C	0.251	101	0.1	0.085	5.09	0.026	27.7	0.019	0.018	0.017	28.2
YF20-039	GUF-39	96.7	6.55 / 23°C	0.189	643	0.08	0.153	3.66	0.036	76.6	0.009	0.012	0.022	10.9
YF20-040	GUF-40	14.8	7.46	0.156	54.8	0	0.036	6.98	0.015	10.4	0.003	0.003	0	14.8
YF20-042	GUF-42	43	7.6	0.222	86.2	0	0.08	6.54	0.022	12.8	0.007	0.006	0	24.3
YF20-043	GUF-43	17.8	8.04	0.203	75.2	0	0.054	10.2	0.022	7.73	0.004	0.036	0.001	16.2
YF20-044	GUF-44	3.4	8.22	Cond	76.7	0	0.023	6.1	0.012	13.5			Ba	Ca

Table 6. (continuation) Chemical components concentration of water samples

Sample	Label	Fe [ppm]	K [ppm]	Mg [ppm]	Mg [ppm]	Mn [ppm]	Na [ppm]	SiO ₂ [ppm]	Sr [ppm]	TDS [ppm]	%_err, Ion_bal ^(a)
YF20-001	ÖLK-01	0.063	0.736	2.24	2.24	0.015	6.63	16.7	0.01	5	0.28
YF20-002	ÖLK-02	<0.001	0.682	1.98	1.98	<0.001	6.43	18.8	0.02	15.2	-4.5
YF20-003	ÖLK-03	65.1	0.697	10.4	10.4	1.82	9.65	44.2	0.07	189	-0.19
YF20-005	REY-05	1.01	10.3	16.0	16.0	0.085	43.8	214.3	0.14	448	3.48
YF20-006	REY-06	0.25	4.94	9.69	9.69	0.057	22.9	110	0.07	222	-2.64
YF20-007	REY-07	0.07	0.804	4.71	4.71	0.035	8.55	31.5	0.03	19	-2.19
YF20-008	REY-08	6.11	4.1	16.0	17.1	0	17.7	90.3	0.06	198	4.84
YF20-010	GRÆ-10	0.001	2.34	2.48	2.48	0.003	37.4	65.3	0.08	173	3.56
YF20-012	REY-12	1	10.4	17.1	17.1	0.088	44.6	217	0.15	492	1.2
YF20-014	REY-14	0.011	0.521	2.90	2.9	0.035	7.09	32.7	0.02	17.3	4.33
YF20-016	GRÆ-16	0.003	1.07	0.89	0.89	0.03	9.44	129	0.04	138	0
YF20-017	GRÆ-17	0.011	0.993	5.86	6.49	0.041	8.63	38.5	0.03	130	0
YF20-022	GRÆ-22	0.024	3.71	0.03	0.026	0.001	58.4	129	0.01	249	1.77
YF20-023	GRÆ-23	0.077	4.23	1.00	0.998	0.054	41.3	107	0.14	219	2.58
YF20-024	GRÆ-24	0.045	1.14	4.92	4.92	0.019	13.9	41.2	0.07	30.4	0.46
YF20-027	GRÆ-27	0.002	2.92	5.13	5.13	0	34.8	83	0.07	46.9	-0.45
YF20-028	GRÆ-28	0.036	2.74	6.86	7.5	0.002	15.5	66.8	0.05	42.6	0.03
YF20-031	GUF-31	0.044	1	3.21	3.21	0.002	8.57	18.6	0.02	16.1	0.79
YF20-032	GUF-32	0.002	1.01	3.14	3.14	<0.001	8.51	18.5	0.02	4.05	-0.14
YF20-033	GUF-33	0.05	2.24	0.20	0.204	0.005	21.7	113	0.01	132	4.01
YF20-034	GUF-34	0.004	2.39	8.51	9.06	0.375	11.5	70.2	0.19	283	-1.75
YF20-035	GUF-35	0.001	0.73	5.44	5.44	<0.001	9.83	17.2	0.07	57.4	-2.77
YF20-037	GUF-37	0.112	3.6	3.06	3.06	0.295	16.7	110	0.13	187	-0.72
YF20-039	GUF-39	3.82	1.05	0.00	6.24	0.252	9.17	141	0.03	227	-2.24
YF20-040	GUF-40	0.003	1.34	3.54	3.54	0.003	10.7	29.9	0.03	47.3	1.79
YF20-042	GUF-42	0.002	2.85	3.16	3.16	<0.001	19	53.1	0.04	104	0.93
YF20-043	GUF-43	0.004	1.71	3.68	3.68	0	22.1	37.5	0.04	84	0.13
YF20-044	GUF-44	0.005	0.722	4.81	4.81	0.003	9.41	22.7	0.05	150	-3.1

^(a) Percent error, expressed as percentual difference of $(Cat-/An)/(Cat+/An)$

The water temperature ranged from 2.2 to 96.7°C and the pH was between 5.45 and 8.38. The sampled waters were characterized by lower Cl concentration between 3.32-10.2 ppm and large range of CO₂ and SO₄ concentration of 6.43-844 ppm and 4.27-111 ppm, respectively. The concentrations of most cations were also very variable, with concentrations ranges of SiO₂ = 16.7-217 ppm, Na = 6.43-58.4 ppm, K = 0.52-10.4 ppm, Mg = 0.03-17.1 ppm, Ca = 2.26-65.7 ppm and Fe = 0.001-65.1 ppm. The results were reported in Table 6.

4.3 Chemical composition of borehole fluids

Several boreholes have been drilled into the geothermal area. Samples of such borehole fluids were not collected and analysed during the field campaign. Instead, recent data from Ölkelduháls and Hveragerði were included (Table 7).

Table 7. Borehole fluids composition from previous studies

Sample	Label	Date sampling	North WGS84	East WGS84	Temp [°C]	Pressure [bar]	Enthalpy [kJ/kg]	Cond [µS/cm]	pH / °C	SiO2 [ppm]	B [ppm]
79-0135 ^(a)	HV-06	28.11.79			158	5.8			9.40 / 19	351	
79-0136 ^(a)	HV-02	28.11.79			148	4.5			9.29 / 19	259	
79-3032 ^(a)	HV-04	18.07.79	64.011	-21.186	164	6.8			8.82 / 20	281	0.62
81-3016 ^(a)	HS-06	19.06.81	63.999	-21.196	180	10			9.50 / 20	442	0.95
81-3017 ^(a)	HS-07	19.06.81	63.996	-21.187	188	12			8.86 / 20	447.2	0.99
B-95809 ^(b)	HS-09	13.11.19	64.005	-21.187	146	3.5	742	725	9.26 / 22	235	0.391
1995-5202 ^(c)	HE-02	30.08.95	64.058	-21.25		3.4		990	9.21 / 24	369.66	
2006-5083 ^(c)	HE-20	30.05.06	64.059	-21.238		5	1059	1190	8.53 / 24	580.1	
2006-5132 ^(c)	HE-22	01.12.06	64.062	-21.255	140	3.2	902		9.23 / 23	442	1.626

Label (continuation...)	Na [ppm]	K [ppm]	Ca [ppm]	Mg [ppm]	Fe [ppm]	Al [ppm]	Cl [ppm]	F [ppm]	CO2 [ppm]	SO4 [ppm]	H2S [ppm]
HV-06	175	18.6	2.35	0			161	0.9	28.5	32.5	
HV-02	168	13.8	2.18	0			142.3	1.7	44.2	40.1	18.4
HV-04	153.3	13.4	1.73	0.002	0.008	0.1	109.5	1.8	74.2	43.7	19.2
HS-06	164.2	20.72	2.15	0.021	0.006		171.2	1	28.6	37.2	23.4
HS-07	176.8	21.28	1.68	0.008	0.005		186.3	0.6	43.4	35.2	23.4
HS-09	170	10.1	2.78	<0.09	0.008	0.4	129	2.1	32.2	64.5	6.2
HE-02	188.34	20.4	1.58	0.002	0.027	0.8	177	0.9	56.4	38.2	18.3
HE-20	235.8	32.71	5.29	0.018	0.053	0.9	233.9	0.7	103	37.1	44.1
HE-22	221.4	24.74	3.16	0.005	0.01	0.9	209.7		24.1	73.1	47.4

(a): Reported: (Stefánsson et al., 2016a)

(b): Reported: (Óskarsson, 2020)

(c): Reported: (Þ. Friðriksson, personal communication, March 4, 2021)

Table 7. (continuation) Borehole fluids composition reported in previous studies

Label	H₂O [μmol/mol]	CO₂ [μmol/mol]	H₂S [μmol/mol]	H₂ [μmol/mol]	CH₄ [μmol/mol]	N₂ [μmol/mol]	O₂ [μmol/mol]	Ar [μmol/mol]
HV-06	999381	239	15.9	19.3	1.22	0	0	0
HV-02	999144	337	16.0	11.6	1.21	0	0	0
HV-04	998222	661	23.5	21.9	2.34	73.6	0	0
HS-06	996838	1015	48.3	23.0	1.55	369	0	5.06
HS-07	996170	1256	109	21.0	2.47	330	0	16.2
HS-09	998363	591	21.8	7.56	1.18	90.0	2.59	1.85
HE-02	999990	11209	76.0	1.87	0.00	7.57	0	0
HE-20	999859	5359	676	105	0.69	33.2	0	2.97
HE-22	999868	2442	101	0	0	130	0	1.85

The liquid phase was characterized by alkaline pH of 8.53-9.50, relatively high Cl concentration of 110-234 ppm, elevated SiO₂ and Na concentration of 235-580 ppm and 153-236 ppm, respectively, low Mg concentration of 0.002-0.020 ppm. The vapor phase is dominated by H₂O with more than 99.9% mol/mol, followed by CO₂, H₂S and H₂ with concentrations of 239-11209 μmol/mol, 15.9-676 μmol/mol and 1,87-105 μmol/mol, respectively. Boreholes distributed in Ölkelduháls present higher non condensable gases concentration than Hveragerði.

5 Discussion

5.1 Reservoir fluid composition

The geothermal reservoir fluid composition was calculated based on chemical composition of two-phase (liquid and steam) borehole discharges (Table 7) using WATCH software as outlined on section 3.4.1. The modelling results are given in Supplement 3. Differences in composition and temperature are observed between areas. The temperature estimation is based on the quartz geothermometer, it lies between 213 and 246°C for Ölkelduháls and between 185 and 235°C for Hveragerði. Total CO₂ is enriched in Ölkelduháls ranging from 1007 to 3816 ppm compared to the average 200 ppm in Hveragerði; same trend is observed in total H₂S. Regarding pH, the primary fluid in Ölkelduháls is slightly acid with pH 5.7 to 6.4 meanwhile Hveragerði is neutral with pH between 5.8 and 7.5. Chloride concentration also differs between both primary fluids, Ölkelduháls present higher concentration (154 – 189 ppm) than Hveragerði (105 – 154 ppm).

5.2 Boiling, steam condensation and mixing process

Reservoir geothermal fluid can undergo changes from depth to surface. These include boiling and formation of boiled liquid and steam, condensation of the steam phase upon cooling, mixing of the boiled liquid and/or steam with non-thermal water and chemical reactions like mineral precipitation and oxidation when in contact with atmospheric oxygen.

Four main type of surface waters can be distinguished in general: 1) Boiled liquid reservoir water typically displaying alkaline pH value and elevated Cl concentration similar to the reservoir fluid, 2) steam heated waters that are formed upon steam condensation and mixing with non-thermal water often followed by oxidation of H₂S to SO₄. Such waters typically display low pH, low Cl concentration and elevated SO₄ concentration, 3) carbonate waters that are formed upon CO₂ mixing and sometimes steam condensation and mixing with non-thermal water. Such waters typically have mildly acid pH, low Cl concentration and elevated CO₂ concentration. 4) non-thermal surface water and groundwater.

The variable end-member waters can be defined or assessed based on reservoir fluid composition, boiled to 100°C and data on steam vent discharges and non-thermal waters. These include boiled reservoir liquid water (brw) and condensed steam (cs) that was estimated based on the adiabatic boiling of the geothermal reservoir fluids to 100°C and 1 bar, corresponding to surface conditions, and non-thermal waters (ntw), represented by the average of 6 rivers samples and 3 cold springs. For the boiled liquid water and condensed steam, the sample HV-06 was used for Hveragerði field and HE-02 for the Ölkelduháls field. A summary of the end-member water compositions is given in Table 8.

Table 8. Composition of water end members, as measured or modeled. Units are in ppm

	Geothermal reservoir water (gr)		Non-thermal waters (ntw)	Boiled reservoir water (brw)		Condensed steam (cs)	
	Hve	Ölk	Average	Hve	Ölk	Hve	Ölk
T [°C]	209	230	6	100	100	100	100
pH	7.40	8.99	7.80	8.55	7.87	2.87	2.67
B	0.554	1.42	0.002	1.14			
SiO ₂	319.8	384.5	29.7	530.1	396.1		
Na	156.8	182.5	9.39	196.9	207.8		
K	14.9	21.4	1.04	24.85	22.5		
Mg	0.01	0.003	3.80	0.025	0.002		
Ca	1.05	1.05	14.65	2.58	1.74		
F	1.278	0.473	0.05	1.15	1.00		
Cl	140	176.6	6.22	205.3	195.3	6.3	6.3
SO ₄	36.7	50.0	13.2	44.6	100	48.8	65.2
Al				0	0.84		
Fe	0.004	0.025	0.03	0.007	0.030		
CO ₂	190.16	2459	48.1	35.4	120	1042	17049
H ₂ S	10.96	32.4		8.84	3.07	95	152

The variable water types may be identified using the relationship between temperature, Cl, SO₄, CO₂ and pH. The samples present low chloride concentration, but often high and variable carbonate and sulphate originating from steam condensate and CO₂ and H₂S gas mixed with non-thermal shallow ground- and surface water followed by oxidation of H₂S to SO₄. Gufudalur hot springs (i.e. GUF-39 and GUF-34) are near neutral pH sulphate (Figure 5c) and Reykjadalur hot springs are near neutral pH carbonate (Figure 5c and 5d); nevertheless, those samples might not be defined as acid steam heated waters since its pH is above 5. Grændalur steam-heated waters present a neutral pH with lower carbonate concentration compared to Reykjadalur. Alternatively, temperature-chloride diagram (Figure 5a) shows low chloride concentration at boiling temperature, typical of condensed steam end member geothermal water (cs). Regarding previous data (Stefánsson et al., 2016a), it includes several acid sulphate waters and boiled hot springs on the vicinity of Varmá river; however, end members components may not have changed during the present survey compared to previous studies.

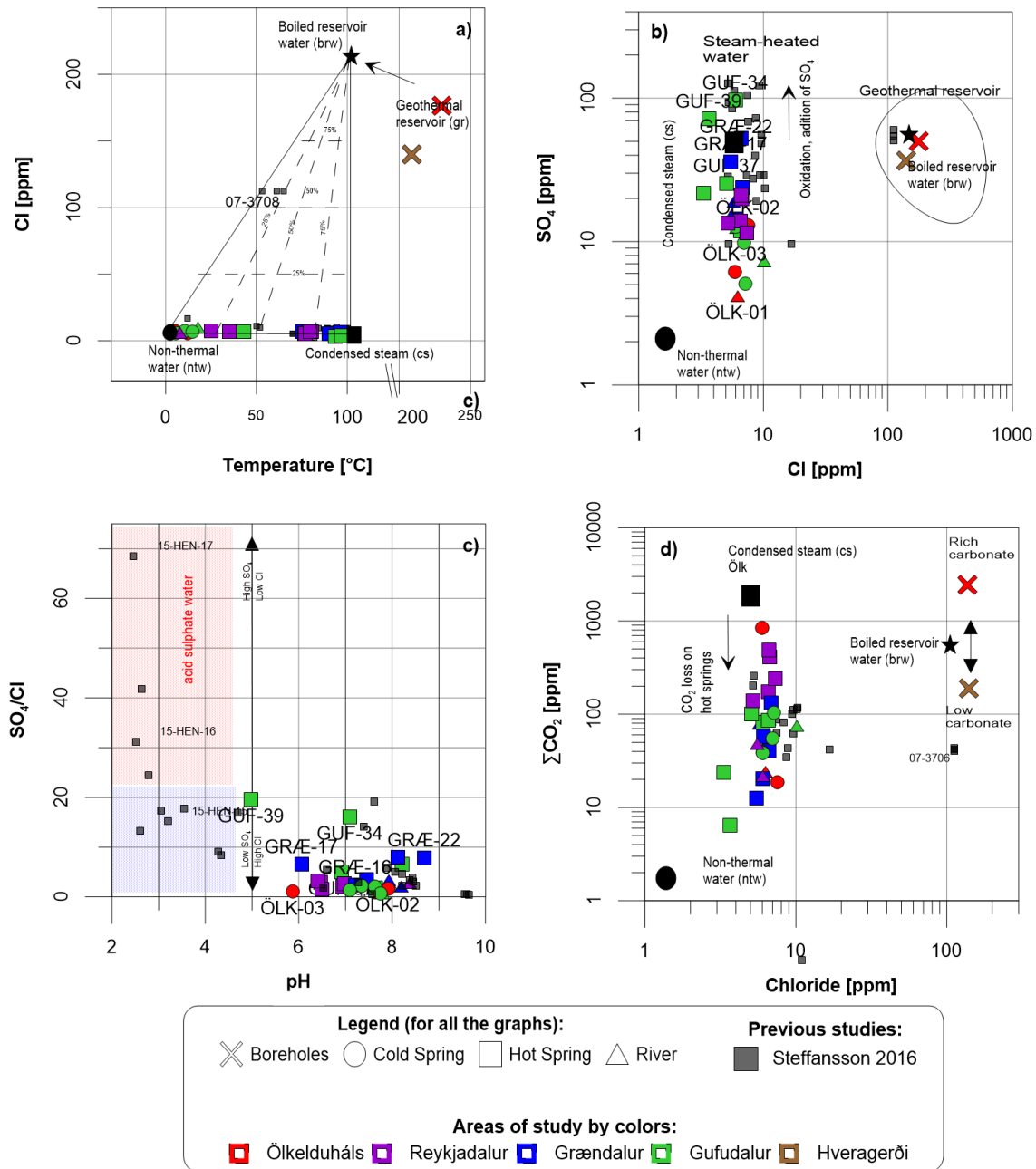


Figure 5. Water classification based on diagrams for: a) Temperature vs. chloride; b) sulphate vs. chloride; c) SO_4/Cl vs. pH and d) HCO_3 vs. chloride.

The oxidation of H_2S to sulfuric acid when exposed to atmospheric oxygen results on the loss of H_2S and the enrichment of SO_4 in steam heated waters and decrease of pH (Steffansson et al., 2016b), this process is observed in GUF-34 where there is an SO_4 addition from 65 ppm to 96 ppm compared to steam condensed end member (Figure 5b). However, the rest of steam heated waters present SO_4 loss compared to the end member, caused by the degassing of H_2S and little oxidation of sulfuric acid, this is also observed on pH ranging from 6 to 9.

Carbon dioxide (CO_2) is largely degassed in steam heated waters (Figure 5d) caused either by the mixing process with non-thermal waters or the degassing of those gases. Carbon

dioxide differs drastically between the steam condensed endmember in Ölkelduháls and Hveragerði with 17049 ppm and 1042 ppm respectively.

Mixing of various water samples for Hveragerði and Ölkelduháls are shown in Figure 6, based on the chloride and temperature diagram. All samples lie on a mixing between non-thermal waters and condensed steam, and no samples belongs to the boiled reservoir water. This diagram also shows that all samples lie in the mixing zone between non-thermal waters and condensed steam. Steam heated water is produced by the condensation of steam vents at surface followed by a different degree mixing with non-thermal waters coming from the shallow and the rainwater. Variations on chloride concentration through the study area are small, between 4 and 10 ppm, mainly explained by the distribution of chloride in non-thermal waters and its variation in precipitation. Rainwater tends to be enriched in chloride on coastal zones and depleted in high ridges.

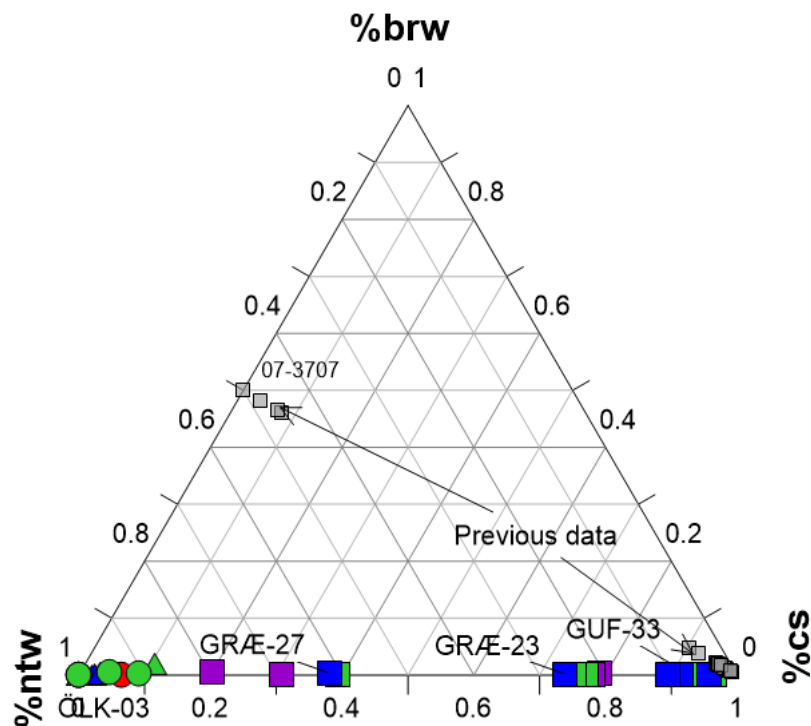


Figure 6. Mixing ratios using the end-member composition: boiler reservoir water (brw), non-thermal waters (ntw) and condensed steam (cs) based on equations (12) to (14).

5.3 Fluid- rock interaction

Boron and chloride are considered conservative elements, meaning that they do not precipitate once added to the fluid phase. The concentrations of chloride and boron are shown in Figure 7a where variations in chloride concentration were observed through the end members: (1) non-thermal waters waters, with low chloride concentration; and (2) geothermal reservoir waters, with more than 10 times higher concentration. Steam heated waters keep similar chloride concentration as surface waters but boron increasing towards bedrock ratio. In general, samples have Cl/B ratio close to the seawater ratio due to the

presence of a small seawater/saline-groundwater component from the hydrogeology of the area. The Cl/B source may come from an initial rainwater composition with addition of atmospheric Cl^- as seawater spray and aerosols, which originally correspond to rain water (Arnórsson & Andrésdóttir, 1995). No evidence of progressive water rock interaction for our dataset was found.

The reaction between the water with the surrounding rocks at surface level may change some components concentrations and can be assessed by those changes in sensitive elements such as SiO_2 , Na, and Mg (Stefánsson et al., 2016b). After depressurization and boiling of the geothermal reservoir, the steam ascends to the surface on both geothermal areas creating condensed steam and dissolving the host rock and eventually form clays. It changes the composition of the steam heated waters suggesting the loss or gain of an element upon ascent to surface.

Significant enrichment of Na, Mg and Fe is observed in the dataset compared to the mixing fractions from chloride and temperature model, the addition of those elements in the water results from the water rock interaction at surface zone with an equilibrium with the host rock and the formation of secondary minerals. Iron is an element that increase its concentration due to the addition of H_2S during degassing. Sample ÖLK-03 presents the highest iron concentration (about 100 ppm) caused by a strong acid leaching between the basalt primary rock and secondary clays (Figure 7c and 7f). It is identified by a coating of the gravel with red-brown iron oxides, and bubbles of CO_2 raising on the water. The second and third highest iron concentrations are found in REY-08 and REY-05 with less than 10 ppm Fe. Minerals in Ölkelduháls contain quartz, anatase, pyrite, smectite, and kaolinite (Kaasalainen & Stefánsson, 2011). Pyrite was the predominant sulfur-bearing mineral reflecting the mobilization of Fe from the host rock (Ludyan, 2020). The total iron concentration is governed by the pH. Iron redox equilibrium is approached with Fe(II) and Fe(III) at $\text{pH} \sim 6$. (Kaasalainen et al., 2017).

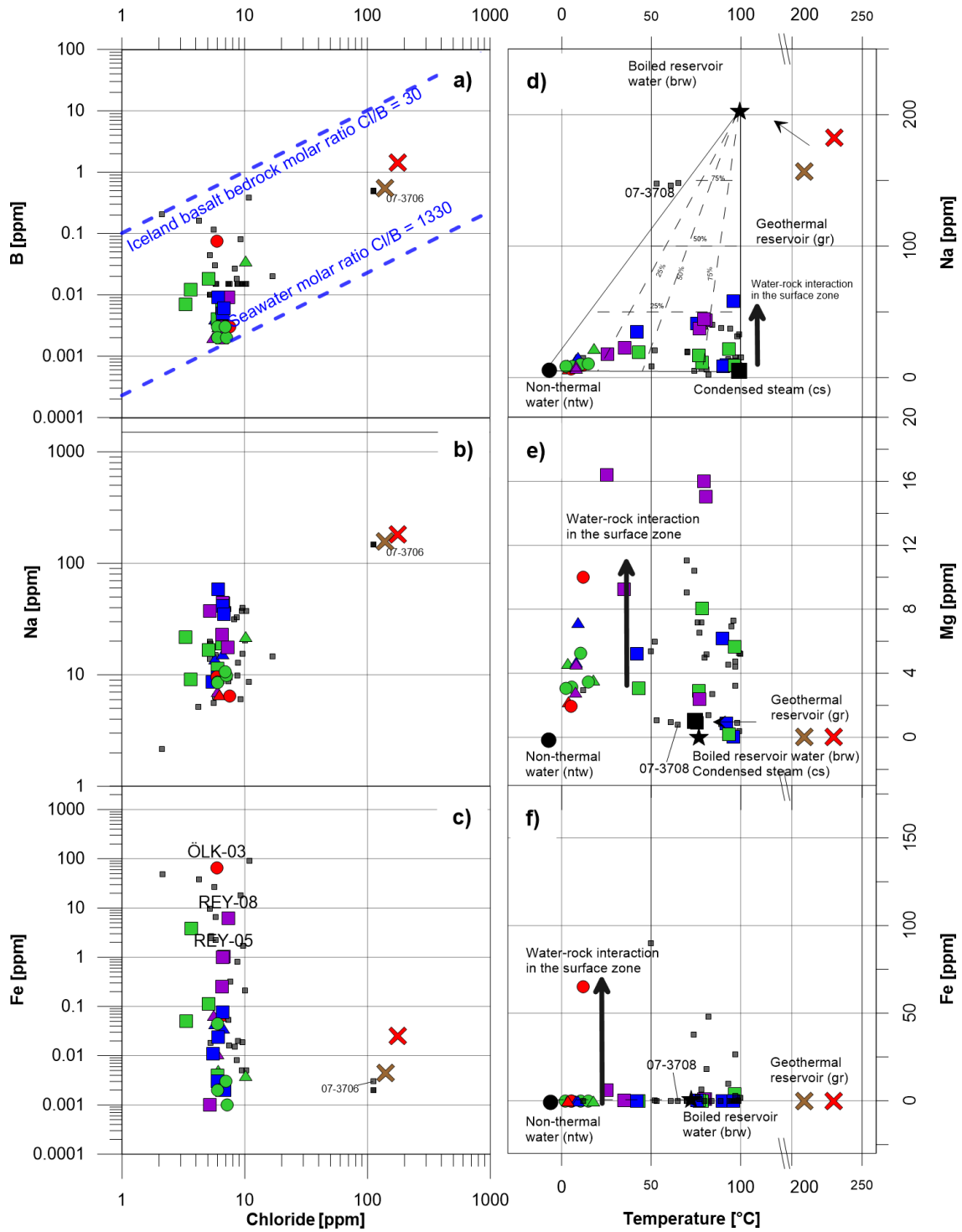


Figure 7. Correlation plots of main constituents, a) chloride vs boron; b) chloride vs sodium; c) chloride vs iron; d) temperature vs sodium; e) temperature vs magnesium; f) temperature vs iron. For explanation of symbols see Figure 5

5.4 Geothermal steam vent discharges

5.4.1 Steam vent composition, boiling, condensation and gas separation

Steam vent fluid composition varies within the area with commonly higher concentrations of CO₂ and H₂S in steam vents in Ölkelduháls, Reykjadalur whereas Grændalur, Gufudalur and Hveragerði have lower CO₂ and H₂S concentrations, generally (Figure 8). These variations may be attributed to the concentration variations in the source fluids, with reservoir fluids at Ölkelduháls having higher CO₂ and H₂S concentrations than in Hveragerði (Supplement 3)

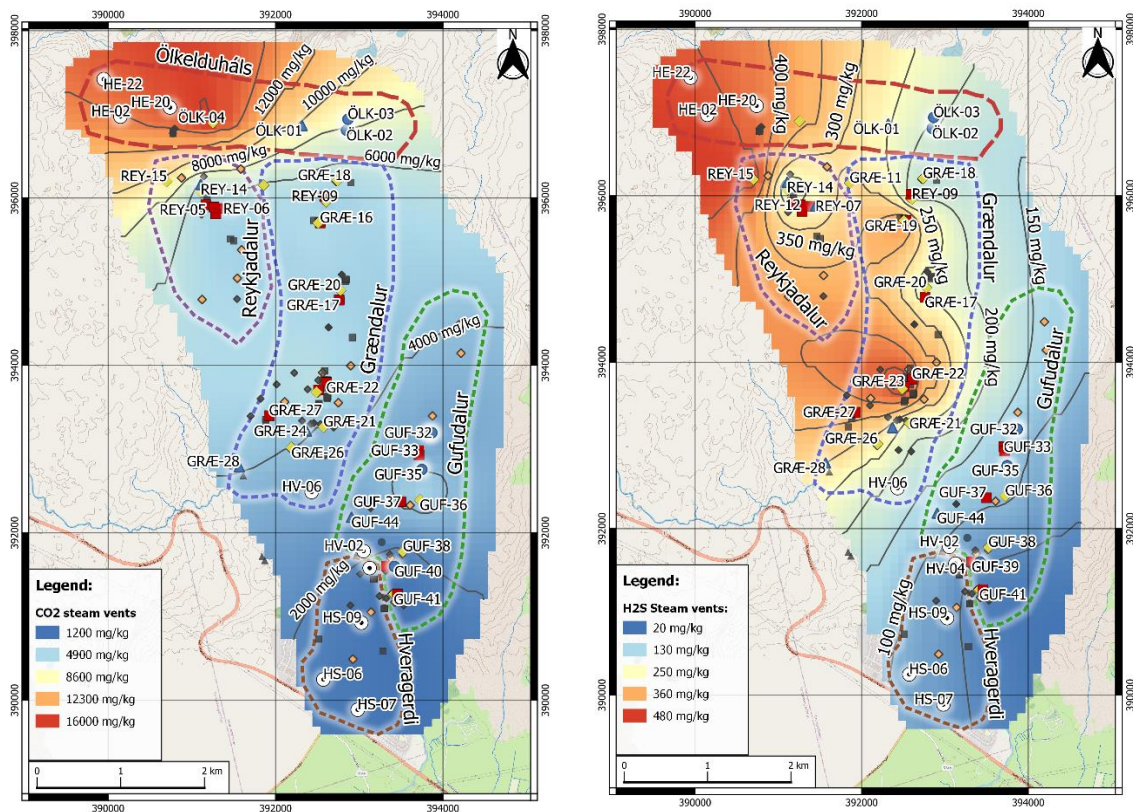


Figure 8. Spatial distribution of a) CO₂ and b) H₂S concentrations measured in steam vents.

Ölkelduháls steam vents and springs present high CO₂ concentration. The source of CO₂ might be related to magma intrusions at depth in Hrómundartindur active volcanic system, where the last magma accumulation happened between 1994-1998 (Clifton et al., 2002). This is also visible on the gas ternary diagrams (Figure 9b and 9c) where the steam vent in the area presents the higher CO₂ concentration on the trend gas addition as well as H₂S compared to N₂ and Ar.

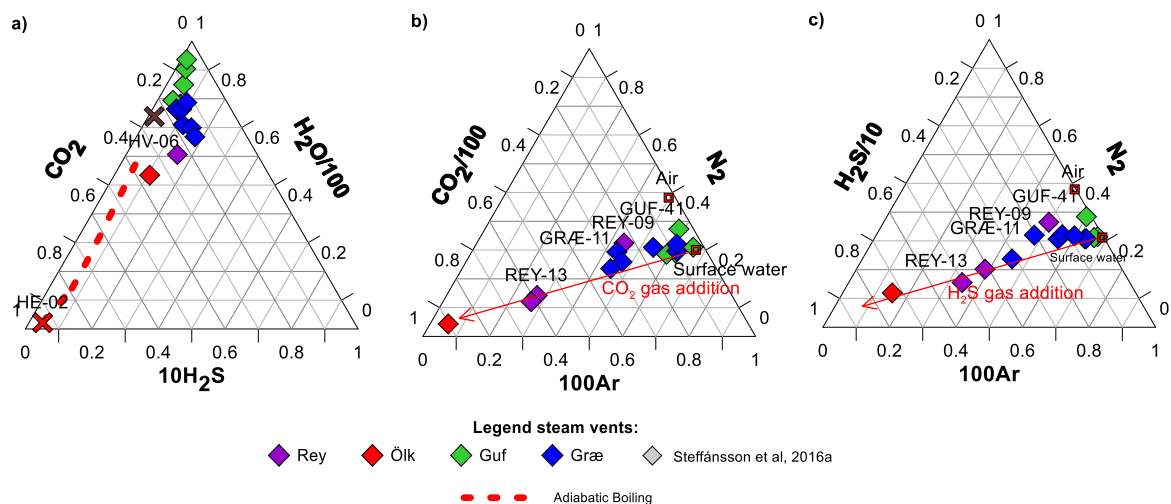


Figure 9. a) H_2O - CO_2 - H_2S gas ternary diagram; b) N_2 - CO_2 -Ar gas ternary diagram, c) N_2 - H_2S -Ar gas ternary diagram.

Nitrogen and argon may further be used to trace possible condensation process that may result in depletion of CO_2 and H_2S in steam vent fluids. Nitrogen is an atmospheric gas derived from the meteoric waters, or of magmatic origin, and Ar is noble gas of atmospheric source used as a conservative species in ratios (Giggenbach, 1986). Nitrogen for the current survey varies from 5 to 172 mg/kg (0.1 to 10 mmol/kg) with the highest concentration in GUF-30; however, the same variation is observed in Argon that goes from 0.09 to 5.22 mg/kg (0.002 to 0.2 mmol/kg) as shown in Figure 10. Those variations follow the meteoric source trend (N_2/Ar molar ratio between 38 to 84) from 46 to 80 which indicates a meteoric source, from no condensation in Ölkelduháls towards a partial condensation of steam in Gufudalur (Figure 10b). The partial condensation in Gufudalur might be caused by (1) conductive heat loss during ascending, or (2) condensation in cooler groundwater/surface water. Regarding air contamination, ÖLK-04, REY-09, GUF-41 and GRÆ-21 show signs of air contamination as shown in Figure 10a; however, it is lower than compared to previous studies in the area and they might consider negligible in the dataset since the highest O_2 concentration found was 3.87 mg/kg (0.1 mmol/kg), as shown in Figure 10a.

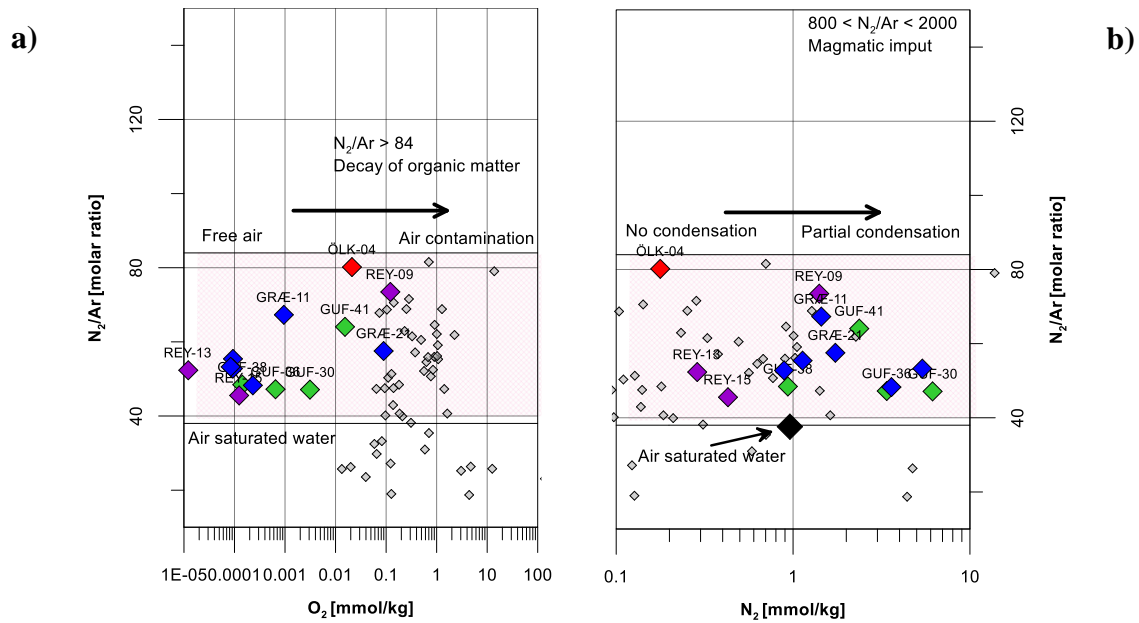


Figure 10. a) N_2/Ar molar ratio – oxygen scatter plot; b) N_2/Ar molar ratio – nitrogen scatter plot. For legend symbol refers to Figure 9.

5.4.2 Gas geothermometry

Gas geothermometers are based on the assumed equilibrium between a gas and a mineral buffer. Gas geothermometers are useful for the estimation of reservoir temperatures in high temperature geothermal systems and the calibrations of (Arnósson & Gunnlaugsson, 1985) are applicable to systems in basaltic host rock like Iceland. The average estimated temperature from the CO_2 , H_2S , H_2 and CO_2/H_2 geothermometers (equations 3 to 7) was used for Ölkelduháls and Reykjadalur areas; however, the possible condensation of the water vapor in the steam during the upflow was considered for Grændalur, Gufudalur and Hveragerði.

The results of gas geothermometry are shown in Supplement 4. The gas temperature estimated shows a lower standard deviation between the geothermometers for Ölkelduháls and Reykjadalur but higher for the south side of Grændalur and Gufudalur, which may be explained by the change of the gas ratios as a larger fraction of the most soluble gases. The water vapor condensation increases the gas concentration on the remaining steam phase and it slightly increases the H_2/CO_2 ratio.

The higher temperatures are found in Ölkelduháls with $297^\circ C$ decreasing towards the south to $230^\circ C$ in Gufudalur. Two temperature reference were found through gas geothermometry, the first one $230-280^\circ C$ in Hveragerdi, and the second one with a temperature range between $280-300^\circ C$ in Ölkelduháls. Gas geothermometry shows about $40^\circ C$ difference in temperatures between both reservoirs but following the same spatial distribution through the four valleys (Figure 11b).

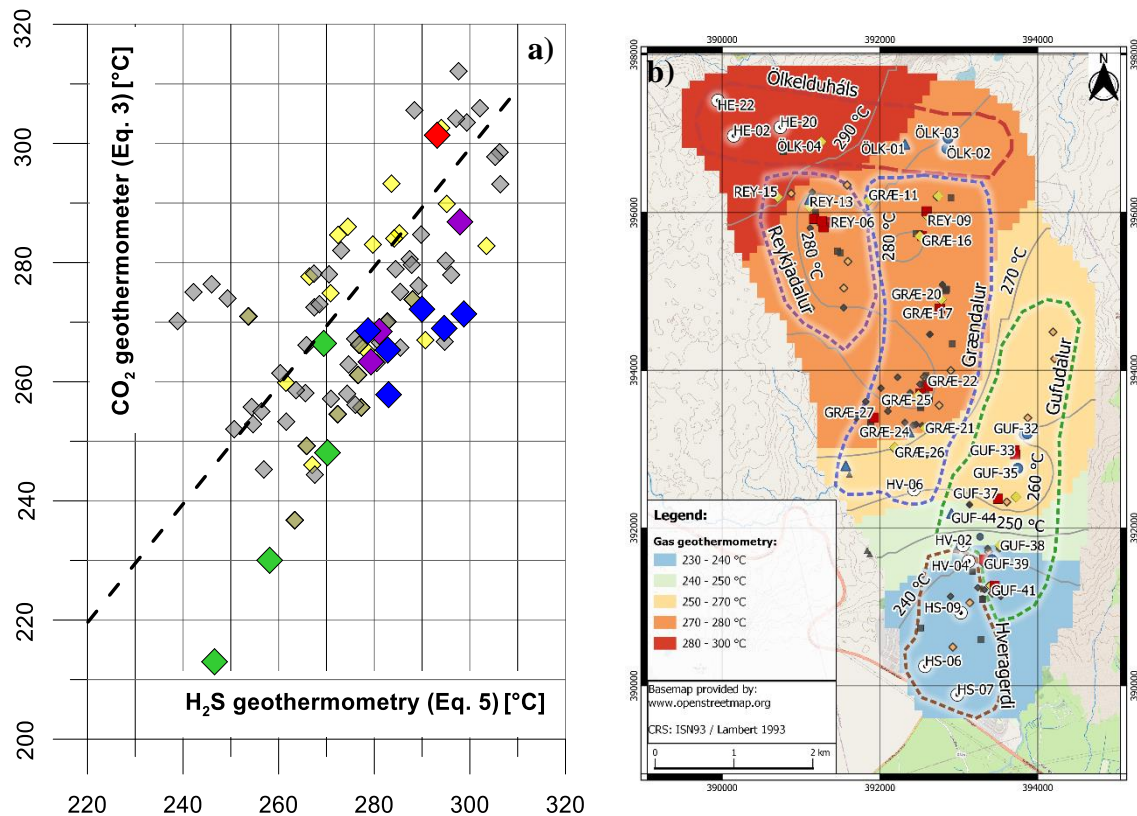


Figure 11. a) Scatter plot of temperatures based in H₂S geothermometer (Eq. 5) and CO₂ geothermometry (Eq. 3); b) Spatial distribution of gas geothermometry for 2020 survey. For symbol legend refers to Figure 9.

5.5 Comparison with previous studies

28 samples of cold springs, hot springs and acid hot springs, 56 steam vents and 5 boreholes sampled through different research from 1982 to 2015 are considered as previous data. Those samples presented characteristics of steam heated waters with Na-HCO₃ and alkaline hot springs around Varmá river and Hveragerði town (Arnórsson & Andrésdóttir, 1995; Arnórsson & Gunnlaugsson, 1985; Kaasalainen & Stefánsson, 2012; Stefánsson, 2017). Steam vents were studied for geothermometry on the areas of Ölkelduháls, Grændalur, Gufudalur (Björnsson, 2007; Ívarsson et al., 2011a).

The chemical characteristics was mainly compared to previous work carried out before the major earthquake event on 29 May 2008. A strong earthquake of Richter scale magnitude 6.3 took place 2 km east of the town of Hveragerði. The earthquake had shallow crustal ruptures, vertical north-south trending, right-lateral strike-slip fault characteristics, similar to other historical events in the past (Halldórsson & Sigbjörnsson, 2009). Several changes related to surface ruptures and geothermal activity were mapped along the area (Eshetu Gemechu, 2017; Kaasalainen & Stefánsson, 2011; Khodayar & Björnsson, 2014).

Alkaline waters may have disappeared on the study area compared to previous data. (Kaasalainen & Stefánsson, 2011) reported 3 samples: 07-3705, 07-3706 and 07-3707 in Gufudalur (Hveragerði down by Laxastigi) with pH of 9.02. The mixing ratio of those samples corresponded to 54% boiled reservoir water and 42% non-thermal water (Figure 6)

becoming the only samples with boiled reservoir end member composition. However, during this study survey all water samples belong to steam heated water with a mixed composition between condensed steam (cs) and non-thermal waters (ntw). The extinction of alkaline waters may have been caused by the opening of new fractures followed by the despresurization of the geothermal reservoir allowing only steam phase reach the surface.

Ívarsson et al., (2011b) studied the gas chemistry and geothermometry of the area based on geochemistry surveys and data available from 1982, 2003, and 2008. The gas composition maintains the same characteristics throughout the study area (Figure 12). The mentioned study also found a discrepancy between the CO₂ and the other geothermometers; thus, the average between H₂S (equation 5) and CO₂ geothermometer (equation 3) were used to quantify the reservoir temperature. For comparison purposes, the same average temperature is used for the current section. The main changes are observed in GRÆ-25 (named GRD-012 in Ívarsson et al., 2011) and GUF-36 (named GUD-002L) with an increase in the estimated reservoir temperature of 21°C and 10°C respectively. However, GUF-41 (named GUD-003) cooled down about 27°C. Regardless of not having a comparison of the ÖLK-04 steam vent, spatial projections based on the gridding method shows an increase of 20°C in Ölkelduháls and decrease of about 20°C in Hveragerði (Figure 11b). It also inferred a fissure NW-SE through steam vents REY-15, REY-13, GRÆ-25 and GUF-36, this signature appears on the spatial distribution of gas geothermometry shown in Figure 13.

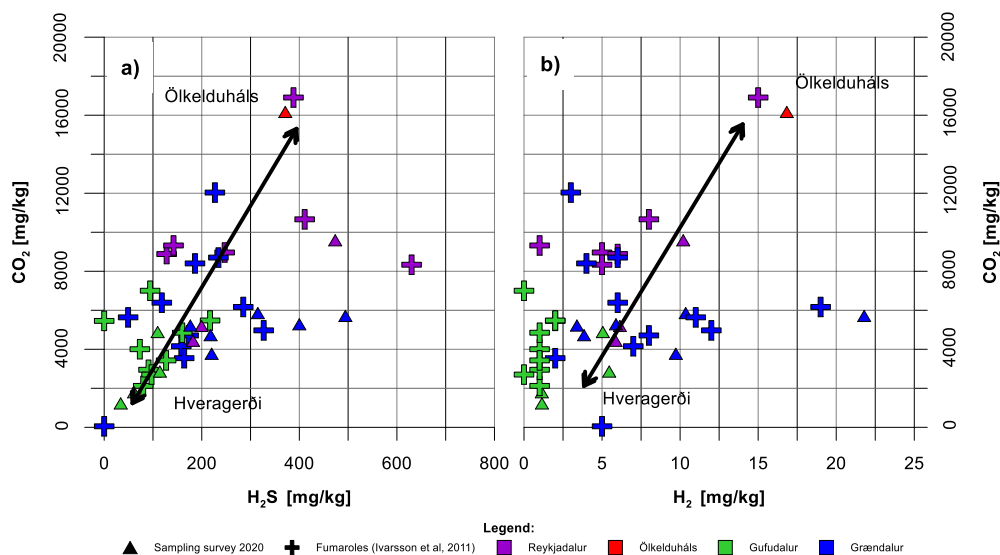


Figure 12. Distribution of a) H₂S and CO₂ gases; b) H₂ and CO₂ gases in steam vents samples and comparison with (Ívarsson et al., 2011b) research.

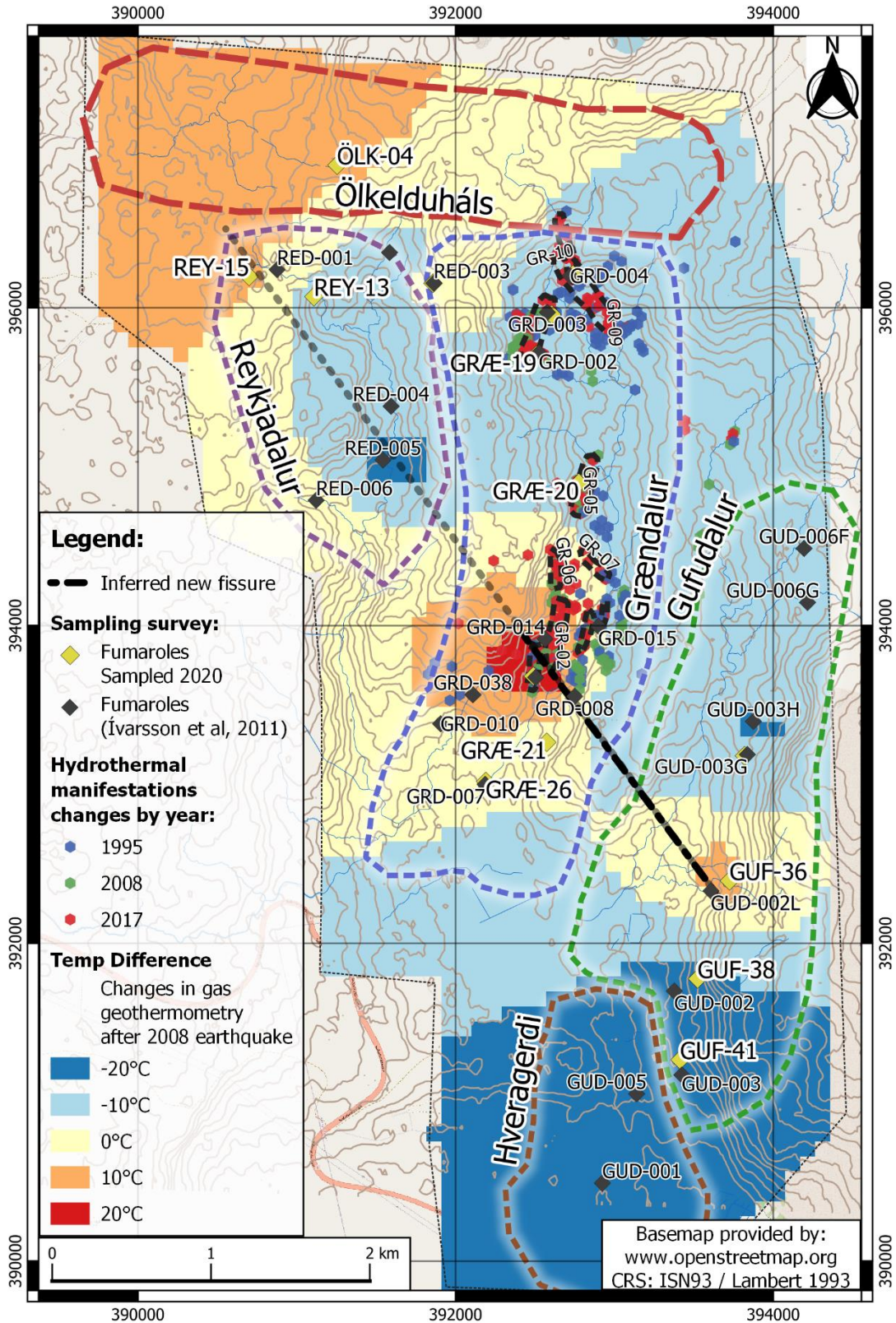


Figure 13. Map of gas geothermometry changes after 2008 earthquake event and comparison of steam vents samples from previous studies (based on Ívarsson et al., 2011)

5.6 Conceptual model

The signatures discussed in the previous section allow for the construction of a conceptual model; however, further research in isotopic geochemistry is needed to define the fluid origin and to track inflow and outflow zones. The conceptual model defines the geothermal reservoir end-members with two primary fluids located in Ölkelduháls and Hveragerði. Major differences in terms of composition are total CO₂ and H₂S where Ölkelduháls is enriched compared to Hveragerði, minor differences are found in SiO₂, and Cl where Ölkelduháls is slightly enriched.

The heat source of the geothermal activity might be controlled by two volcanic systems. On the north, Hrómundartindur active volcanic system supplies heat to Ölkelduháls where the estimated temperature is 280-300°C. In the south, Grændalur extinct volcano supplies heat to Hveragerði and Gufudalur where the estimated temperature is 230-280°C. The interface between that two end-members reservoirs are Reykjadalur and Grændalur that are mainly defined by steam heated waters that are formed by mixing between condensed steam and nonthermal waters.

Both geothermal areas present secondary fluids on surface as steam heated waters and steam vents; although no alkaline springs were found during the 2020 survey, previous data shows boiling hot springs in Hveragerði by the Varmá river. Ölkelduháls wells and steam vents have higher CO₂ and H₂S concentration than Hveragerði; however, chloride concentration is higher in Hveragerði. As observed by Arnórsson & Andrésdóttir, (1995), the higher chloride concentration may be due to the presence of a seawater source. Regarding steam vents, partial condensation was observed in Gufudalur, most probably caused by the conductive cooling of the fluid during ascending. The extent of partial condensation is reduced throughout Grændalur and Gufudalur to reach Ölkelduháls defined as no condensation.

Steam-heated waters are distributed over the three valleys. Those fluids contain dissolved CO₂ and SO₄ (from H₂S) carried by the steam. Figure 14 shows the fluid ascension from the reservoir to the surface, Ölkelduháls presents no water condensation during boiling but Hveragerði presents partial water condensation, this process is followed by a mixing process with non-thermal water mainly from shallow ground water. Although no evidence of progressive water rock interaction was found, a certain level of water rock interaction in the surface zone is governed by the CO₂ and H₂S degassing and the alteration of the hostrock. This process is highlighted in Ölkelduháls but not observed in Hveragerði. Additionally, steam heated waters and nonthermal waters in Ölkelduháls and Reykjadalur have lower pH (i.e ÖLK-03 with pH 5,4 and REY-05 with pH 6,25) due to the degassing and oxidation of H₂S towards SO₄, and the alteration process of the host rock basalt/hyaloclastite towards clays like smectite/kaolinite and pyrite (Ludyan, 2020), it results in high concentrations of H₂S and CO₂ gases and the sulfur oxidation states in most natural geothermal waters (Kaasalainen & Stefánsson, 2011).

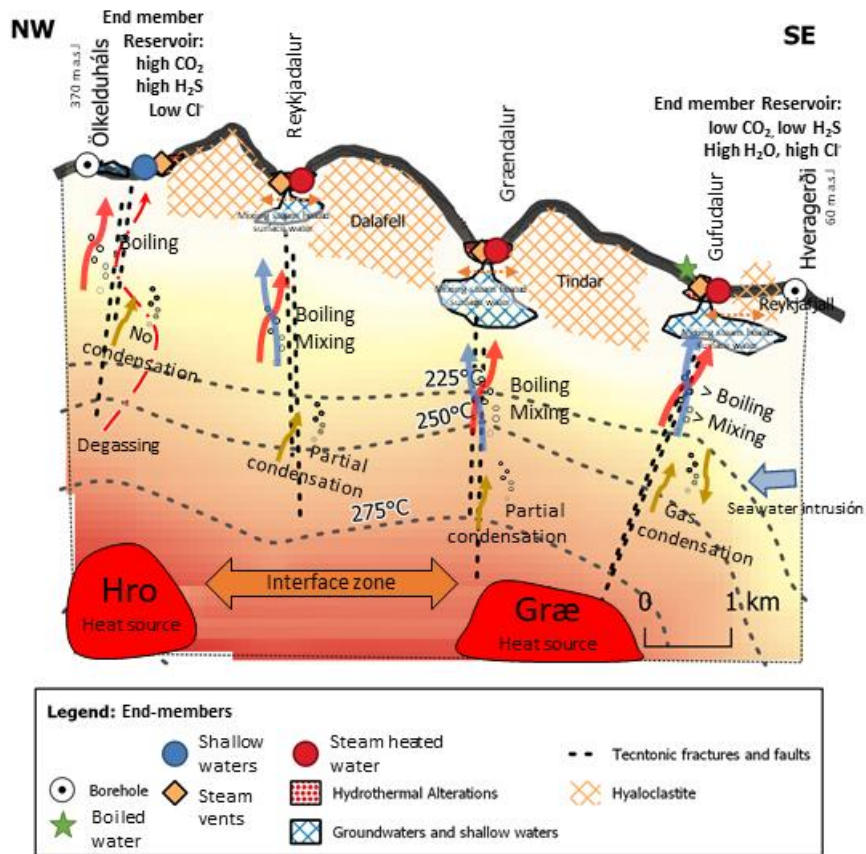


Figure 14. Schematic conceptual model of the the study area (based in Geirsson & Arnórsson, 1995).

6 Conclusions

Samples from geothermal manifestations in five subareas of the Ölkelduháls and Hveragerði geothermal fields were analyzed and classified according to their water and gas chemistry. The temperature of the geothermal reservoir was estimated through gas geothermometry giving a temperature of 230-280°C in Hveragerði and 280-300°C in Ölkelduháls. This estimation shows higher temperature than the measured temperature on Hveragerði geothermal wells, which range from 215°C to 230°C, and 256°C in the HE-20 geothermal well of Ölkelduháls (Björnsson, 2007; Geirsson & Arnórsson, 1995).

The water manifestations are steam heated water with a different degree of mixing between the condensed steam (sc) and non-thermal waters (ntw) end members, no alkaline hot springs were found during the 2020 survey although previous data asseverates the presence of boiled hot springs with a mixing degree of boiled reservoir water (brw) and non-thermal waters.

Gas chemistry indicates that Ölkelduháls is enriched in CO₂ and H₂S compared to Hveragerði. Their source may be related to magma intrusions at depth in Hrómundartindur active volcanic system, Nitrogen and N₂/Ar ratio shows meteoric air source with no condensation in Ölkelduháls and steam condensation in Hveragerði during boiling.

The heat source of the geothermal activity might be controlled by two volcanic systems. On the north Hrómundartindur supplies heat to Ölkelduháls; in the south, Grændalur extinct volcano supplies heat to Hveragerði and Gufudalur. The interface between the two primary fluids are Reykjadalur and Grændalur that are mainly defined by steam vents and steam heated waters. Steam vents on those areas resemble CO₂, H₂S and H₂ concentration on the middle of both end-member composition that might suggest a shared composition of both primary fluids.

H₂S and CO₂ concentration in steam vents kept the same characteristics after the 2008 seismic event although new outflow zones appeared. The seismic event either open and close fractures or faults rupture and it affected the appearance of geothermal manifestations. However, the primary and secondary fluids of geothermal areas are rather governed by the heat source, mixing of condensed steam and non-thermal waters, water-rock interaction in the surface zone, gas-mineral and gas-gas interaction.

References

- Ármannsson, H. (2016). The fluid geochemistry of Icelandic high temperature geothermal areas. *Applied Geochemistry*, 66, 14–64. <https://doi.org/10.1016/j.apgeochem.2015.10.008>
- Árnason, K., Haraldsson, G., Johnsen, G., Hersir, G. P., Saemundsson, K., Georgsson, L., & Snorrason, S. (1986). *Nesjavellir: Jarðfræði- og jarðeðlisfræðileg könnun 1985* (OS-86014/JHD-02; p. 125). Orkustofnun. <https://orkustofnun.is/gogn/Skyrslur/OS-1986/OS-86014.pdf>
- Arnórsson, S., & Andrésdóttir, A. (1995). Processes controlling the distribution of boron and chlorine in natural waters in Iceland. *Geochimica et Cosmochimica Acta*, 59(20), 4125–4146. [https://doi.org/10.1016/0016-7037\(95\)00278-8](https://doi.org/10.1016/0016-7037(95)00278-8)
- Arnórsson, S., Bjarnason, J. Ö., Giroud, N., Gunnarsson, I., & Stefánsson, A. (2006). Sampling and analysis of geothermal fluids. *Geofluids*, 6(3), 203–216. <https://doi.org/10.1111/j.1468-8123.2006.00147.x>
- Arnórsson, S., & Gunnlaugsson, E. (1985). New gas geothermometers for geothermal exploration—Calibration and application. *Geochimica et Cosmochimica Acta*, 49(6), 1307–1325. [https://doi.org/10.1016/0016-7037\(85\)90283-2](https://doi.org/10.1016/0016-7037(85)90283-2)
- Arnórsson, S., Stefánsson, A., & Bjarnason, J. Ö. (2007). Fluid-fluid interactions in geothermal systems. *Reviews in Mineralogy and Geochemistry*, 65, 259–312. Scopus. <https://doi.org/10.2138/rmg.2007.65.9>
- Bjarnason, J. (2010). *The chemical speciation program WATCH, version 2.4* (p. 9). Iceland GeoSurvey (ÍSOR). <https://en.isor.is/software>
- Björnsson, G. (2007). *Endurskoðað hugmyndafræðingur af jarðhitakerfum í Hengli og einfalt mat á vinnslugetu nýrra borsvæða* (OR-2007-3). Orkuveita Reykjavíkur.
- Bodvarsson, G. (1961). Physical characteristics of natural heat resources in Iceland. *Jökull*, 11, 29–38.
- Bragadóttir, R. B. (2019). *Numerical modelling of the Hveragerði high temperature field* [Thesis, Reykjavík University]. <https://skemman.is/handle/1946/33821>
- Clifton, A. E., Sigmundsson, F., Feigl, K. L., Gunnar Guðmundsson, & Árnadóttir, T. (2002). Surface effects of faulting and deformation resulting from magma accumulation at the Hengill triple junction, SW Iceland, 1994–1998. *Journal of*

Volcanology and Geothermal Research, 115(1), 233–255.
[https://doi.org/10.1016/S0377-0273\(01\)00319-5](https://doi.org/10.1016/S0377-0273(01)00319-5)

Eshetu Gemechu, A. (2017). *Geothermal exploration in Graendalur valley, Hveragerdi, S-Iceland* (UNU Geothermal Training Programme No. 11; pp. 113–134). Orkustofnun. <http://hdl.handle.net/10802/16641>

Fridleifsson, I. B. (1979). Geothermal activity in Iceland. *Jökull*, 29, 47–56. Scopus.

Friðriksson, Þ. (2021, March 4). *Chemical analysis on three boreholes in Ölkelduháls provided by Reykjavik Energy (Orkuveita Reykjavíkur)* [Personal email].

Geirsson, K., & Arnórsson, S. (1995). *Conceptual model of the Hveragerdi geothermal reservoir based on geochemical data*. 1251–1256.

Gestsdóttur, K., & Geirsson, K. (1990). Chemistry of thermal waters in the Hveragerdi geothermal field. *Unpublished Report (in Icelandic)*. University of Iceland, Reykjavik, 90pp.

Giggenbach, W. F. (1986). The use of gas chemistry in delineating the origin of fluids discharged over the Taupo Volcanic Zone. *Proceedings of Symposium 5, Int. Volc. Congress, Auckland*, 47–50.

Gudmundsson, O., & Brandsdóttir, B. (2010). Geothermal noise at Olkelduhals, SW Iceland. *Jökull*, 60, 89–102.

Halldórsson, B., & Sigbjörnsson, R. (2009). The Mw6.3 Ölfus earthquake at 15:45 UTC on 29 May 2008 in South Iceland: ICEARRAY strong-motion recordings. *Soil Dynamics and Earthquake Engineering*, 29(6), 1073–1083. <https://doi.org/10.1016/j.soildyn.2008.12.006>

Ívarsson, G. (1998). Fumarole gas geochemistry in estimating subsurface temperatures at Hengill in Southwestern Iceland, International symposium; 9th, Water-rock interaction. *Water-Rock Interaction, International Symposium; 9th, Water-Rock Interaction*, 9, 459–462. <https://www.tib.eu/de/suchen/id/BLCP%3ACN023965477>

Ívarsson, G., Sigurðardóttir, Á., Kristinsdóttir, B., Þrastarson, E. Ö., Gretarsson, S., & Þorsteinsson, Þ. (2011a). *Yfirborðsjarðhiti á Hengilssvæðinu IV* ([Surface Geothermal Heat in the Hengill Area Tech. Rep. 2011-34). Orkuveita Reykjavíkur.

Ívarsson, G., Sigurðardóttir, Á., Kristinsdóttir, B., Þrastarson, E. Ö., Gretarsson, S., & Þorsteinsson, Þ. (2011b). *Yfirborðsjarðhiti á Hengilssvæðinu IV* (No. 2011–34; p. 224). Orkuveita Reykjavíkur.

- Kaasalainen, H., & Stefánsson, A. (2011). Sulfur speciation in natural hydrothermal waters, Iceland. *Geochimica et Cosmochimica Acta*, 75(10), 2777–2791. <https://doi.org/10.1016/j.gca.2011.02.036>
- Kaasalainen, H., & Stefánsson, A. (2012). The chemistry of trace elements in surface geothermal waters and steam, Iceland. *Chemical Geology*, 330–331, 60–85. <https://doi.org/10.1016/j.chemgeo.2012.08.019>
- Kaasalainen, H., Stefánsson, A., & Druschel, G. K. (2017). Geochemistry and speciation of Fe(II) and Fe(III) in natural geothermal water, Iceland. *Applied Geochemistry*, 87, 146–157. <https://doi.org/10.1016/j.apgeochem.2017.10.021>
- Kaasalainen, H., Stefánsson, A., Giroud, N., & Arnórsson, S. (2015). The geochemistry of trace elements in geothermal fluids, Iceland. *Applied Geochemistry*, 62, 207–223. <https://doi.org/10.1016/j.apgeochem.2015.02.003>
- Khodayar, M., & Björnsson, S. (2014). Fault ruptures and geothermal effects of the second earthquake, 29 May 2008, South Iceland Seismic Zone. *Geothermics*, 50, 44–65. <https://doi.org/10.1016/j.geothermics.2013.07.002>
- Kyagulanyi, D. (1996). *Geothermal exploration in the Hveragerdi-Graendalur area, SW-Iceland* (No. 8; UNU Geothermal Training Programme, pp. 161–176). United Nations University. <https://orkustofnun.is/gogn/flytja/JHS-Skjol/Yearbook1996/1996-08.pdf>
- Ludyan, J. (2020). Surface Alteration in the Ölkelduháls, Nesjavellir, and Geysir Hydrothermal Systems, Iceland: Implications for Mars. *Theses and Dissertations*. <https://dc.uwm.edu/etd/2553>
- Malik, A. H. (1996). *Geothermal exploration of Saudá Valley North of Hveragerdi, SW-Iceland* (1996 No. 9; UNU Geothermal Training Programme, pp. 177–195). United Nations University. <https://orkustofnun.is/gogn/unu-gtp-report/UNU-GTP-1996-09.pdf>
- Mutonga, M. W. (2007). *The isotopic and chemical characteristics of geothermal fluids in Hengill area, SW-Iceland: Hellisheidi, Hveragerdi and Nesjavellir fields* (UNU Geothermal Training Programme No. 15; pp. 333–370). United Nations University.
- Natukunda, J. F. (2005). *Geothermal exploration in eastern Ölkelduháls field, Hengill area, SW-Iceland* (UNU Geothermal Training Programme No. 14; pp. 247–264). United Nations University. <https://orkustofnun.is/gogn/unu-gtp-report/UNU-GTP-2005-14.pdf>
- Okedi, J. P. O. (2006). *Reservoir evaluation of the Ölkelduháls geothermal field, Hengill area, SW-Iceland* (UNU Geothermal Training Programme No. 16; pp. 315–355).

- United Nations University. <https://orkustofnun.is/gogn/unu-gtp-report/UNU-GTP-2006-16.pdf>
- Óskarsson, F. (2020). *Chemical composition of fluids from well HS-09 in Hveragerði* (ÍSOR-20001; p. 5). Iceland GeoSurvey (ÍSOR).
- Ragnarsson, Á., Steingrímsson, B., & Thorhallsson, S. (2021). Geothermal Development in Iceland 2015-2019. *World Geothermal Congress 2020+1*. Session 50A, Reykjavik. <https://pangea.stanford.edu/ERE/db/WGC/papers/WGC/2020/01063.pdf>
- Richter, B., Steingrímsson, B., Ólafsson, M., & Karlsdóttir, R. (2010). Geothermal Surface Exploration in Iceland. *World Geothermal Congress 2010*, 6.
- Sæmundsson, K. (1979). Outline of the geology of Iceland. *Jokull*, 29, 7–28.
- Sæmundsson, K., Jóhannesson, H., Hjartarson, Á., Kristinsson, S. G., & Sigurgeirsson, M. A. (2010). Geological Map of Southwest Iceland, 1: 100 000. *Iceland GeoSurvey*.
- Stefánsson, A. (2017). Gas chemistry of Icelandic thermal fluids. *Journal of Volcanology and Geothermal Research*, 346, 81–94. <https://doi.org/10.1016/j.jvolgeores.2017.04.002>
- Stefánsson, A., Arnórsson, S., Kjartansdóttir, R., Gunnarsson Robin, J., Sveinbjörnsdóttir, Á., Kaasalainen, H., & Keller, N. S. (2016a). GeoFluids database 2016: Chemical composition of Icelandic fluids and gases. In *Sci. Inst. Report RH-10-2016*.
- Stefánsson, A., Keller, N., Robin, J. G., Kaasalainen, H., Björnsdóttir, S., Pétursdóttir, S., Jóhannesson, H., & Hreggvidsson, G. Ó. (2016b). Quantifying mixing, boiling, degassing, oxidation and reactivity of thermal waters at Vonarskard, Iceland. *Journal of Volcanology and Geothermal Research*, 309, 53–62. <https://doi.org/10.1016/j.jvolgeores.2015.10.014>
- Steigerwald, L., Einarsson, P., & Hjartardóttir, Á. R. (2020). Fault kinematics at the Hengill Triple Junction, SW-Iceland, derived from surface fracture pattern. *Journal of Volcanology and Geothermal Research*, 391, 106439. <https://doi.org/10.1016/j.jvolgeores.2018.08.017>
- Steingrímsson, B. (2014). Phases of geothermal development in Iceland: From a hot spring to utilization. *Short Course VI on Utilization of Low- and Medium-Enthalpy Geothermal Resources and Financial Aspects of Utilization*. Phases of geothermal development, El Salvador.
- Walker, C. L. (1992). *The volcanic history and geochemical evolution of the Hveragerði Region, S. W. Iceland*. [Doctoral, Durham University]. https://doi.org/10.1/5610_3026.PDF

Xi-Xiang, Z. (1980). *Interpretation of Subsurface Temperature Measurements in the Mosfellssveit and Olfusdalur Geothermal Areas, SW-Iceland* (UNU Geothermal Training Programme No. 1980-07; Issue 7). Orkustofnun.

Zhanxue, S., & Linchuan, J. (1998). *Geothermometry and chemical equilibria of geothermal fluids from Hveragerdi, SW-Iceland, and selected hot springs Jiangxi province, SE-China*. United Nations University.

Supplement 1: Chemical composition of steam vents from previous studies

Table S1.1. The chemical composition of steam vents in Iceland, units are expressed in $\mu\text{mol/mol}$ total fluid. (Stefánsson et al., 2016a)

Report ID	Date	Area	Coordinates, WGS84		H ₂ O	CO ₂	H ₂ S	H ₂	CH ₄	O ₂	N ₂	Ar
			North	South								
82-3028	05/06/1982	Reykjadalur	64.0228	-21.1971	997882	1814	103	76	3.49	0.00	118	4.03
82-3029	05/06/1982	Reykjadalur	64.0228	-21.1971	997491	2054	81	67	2.34	10.57	284	9.17
82-3030	05/06/1982	Reykjadalur	64.0261	-21.1986	997773	1963	132	56	3.15	0.00	70	2.94
82-3031	05/06/1982	Reykjadalur	64.0308	-21.1995	996974	2536	151	170	3.04	1.06	160	4.94
82-3032	05/06/1982	Reykjadalur	64.0298	-21.2020	997435	2315	26	99	2.85	0.36	117	4.47
82-3041	09/06/1982	Grændalsá	64.0264	-21.2031	996847	2738	161	150	3.54	0.00	96	4.41
82-3037	09/06/1982	Gufudalur	64.0173	-21.1856	998784	1062	53	1.3	0.00	12.69	84	2.38
82-3038	09/06/1982	Gufudalur	64.0173	-21.1856	997518	2241	114	19	3.56	0.24	100	3.91
82-3039	09/06/1982	Gufudalur	64.0173	-21.1856	997527	2251	115	18	2.89	0.00	83	3.06
82-3040	09/06/1982	Reykjadalur	64.0262	-21.2127	998181	1694	75	8	0.29	3.49	37	1.30
82-3042	09/06/1982	Reykjadalur	64.0315	-21.2054	996400	2928	52	42	0.00	85.81	474	17.97
82-3043	09/06/1982	Reykjadalur	64.0302	-21.2096	997322	2552	21	56	1.37	0.00	40	7.23
82-3073	21/06/1982	Grændalsá			997844	1452	87	17	0.97	79.70	493	26.36
82-3074	21/06/1982	Grændalsá			998135	1472	82	19	0.95	0.00	292	0.00
82-3075	21/06/1982	Grænsdalur	64.0365	-21.1974	996603	3179	146	39	1.21	3.26	28	0.58
82-3076	21/06/1982	Grænsdalur	64.0365	-21.1974	991938	7812	155	33	4.34	2.24	53	1.95
82-3077	21/06/1982	Grænsdalur	64.0365	-21.1974	997835	1988	48	19	0.38	10.17	98	1.88
82-3079	21/06/1982	Grænsdalur	64.0365	-21.1974	997119	2643	132	32	0.79	1.16	70	1.47
82-3080	21/06/1982	Grænsdalur	64.0365	-21.1974	996689	3080	150	37	0.76	1.49	41	1.23
82-3071	21/06/1982	Gufudalur			998331	1554	75	5.9	0.27	2.49	31	0.72
82-3067	21/06/1982	Hveragerði	64.0102	-21.1876	998465	1407	68	6.2	1.05	1.75	51	1.27
82-3068	21/06/1982	Hveragerði	64.0068	-21.1897	999050	872	43	7.0	0.34	1.17	26	0.88
82-3069	21/06/1982	Hveragerði	64.0079	-21.1827	998560	1211	48	6.7	0.99	13.88	156	3.08
82-3083	21/06/1982	Ölkelduháls	64.0567	-21.2371	991910	7412	243	98	4.93	41.25	287	4.64
82-3084	21/06/1982	Ölkelduháls	64.0567	-21.2371	989171	9984	250	213	17.43	25.89	332	7.03

Table S1.1. (...continuation) The chemical composition of steam vents in Iceland, units are expressed in $\mu\text{mol/mol}$ total fluid. (Stefánsson et al., 2016a)

Report ID	Date	Area	Coordinates, WGS84		H ₂ O	CO ₂	H ₂ S	H ₂	CH ₄	O ₂	N ₂	Ar
			North	South								
82-3078	21/06/1982	Reykjadalur	64.0392	-21.2200	997798	2015	106	16	0.49	0.00	60	4.12
82-3072	26/06/1982	Gufudalur			997857	1991	85	9.2	0.70	3.34	52	1.28
14-HVG-13	20/05/2014	Hellisheiði	64.0200	-21.3955	993427	5569	692	180	18.93	4.45	107	1.61
14-HVG-04	20/05/2014	Hveragerði	64.0077	-21.1810	998555	1309	22	6.6	0.39	19.36	86	1.55
14-HVG-05	20/05/2014	Hveragerði	64.0082	-21.1798	998522	1342	27	6.2	0.18	16.46	85	1.31
14-HVG-06	20/05/2014	Hveragerði	64.0083	-21.1792	998798	1087	30	6.5	0.00	11.32	65	1.19
14-HVG-07	20/05/2014	Hveragerði	64.0081	-21.1792	998417	1456	27	6.7	0.43	16.25	76	1.35
14-HVG-08	20/05/2014	Hveragerði	64.0070	-21.1767	998439	1425	30	10	0.54	15.29	80	1.52
14-HVG-09	20/05/2014	Hveragerði	64.0124	-21.1775	998543	1357	39	10	0.40	6.79	44	0.77
14-HVG-10	20/05/2014	Hveragerði	64.0124	-21.1775	998277	1559	48	13	0.57	18.55	84	1.49
14-HVG-11	20/05/2014	Hveragerði	64.0106	-21.1814	998098	1722	36	11	1.01	12.25	117	2.10
14-HVG-12	20/05/2014	Hveragerði	64.0124	-21.1805	998290	1582	43	15	0.89	2.30	66	1.28
14-HVG-01	20/05/2014	Ölkelduháls	64.0571	-21.2370	993412	6014	387	105	3.28	4.59	73	1.06
14-HVG-02	20/05/2014	Ölkelduháls	64.0572	-21.2367	994508	4944	389	97	2.64	5.15	53	0.74
14-HVG-03	20/05/2014	Ölkelduháls	64.0571	-21.2370	993625	5848	369	103	3.25	1.34	50	0.74
14-HVG-14	06/06/2014	Grænsdalur	64.0422	-21.1946	996837	2916	62	92	2.67	4.21	85	1.35
14-HVG-15	06/06/2014	Grænsdalur	64.0422	-21.1946	996398	3342	70	92	2.58	5.93	88	1.43
14-HVG-17	06/06/2014	Grænsdalur	64.0258	-21.1953	996461	2259	12	8.0	2.54	249.52	996	12.60
14-HVG-18	06/06/2014	Grænsdalur	64.0258	-21.1953	997607	2024	213	10	2.80	19.03	122	2.06
14-HVG-20	06/06/2014	Grænsdalur	64.0229	-21.2002	997287	2430	52	63	1.47	23.09	141	2.05
14-HVG-21	06/06/2014	Grænsdalur	64.0229	-21.2002	997319	2472	55	67	1.34	8.90	74	1.23
14-HVG-22	06/06/2014	Grænsdalur	64.0262	-21.2002	997045	2758	17	64	1.49	18.21	93	1.50
14-HVG-23	06/06/2014	Grænsdalur	64.0262	-21.2002	997178	2641	14	54	1.27	12.68	98	1.20
14-HVG-24	06/06/2014	Grænsdalur	64.0261	-21.2009	996416	3148	216	138	2.27	2.57	76	1.07
14-HVG-25	06/06/2014	Grænsdalur	64.0261	-21.2009	996485	2907	229	247	4.48	1.88	124	1.80

Table S1.2. The chemical composition of steam vents, units are expressed in $\mu\text{mol/mol}$ total fluid. (Ívarsson et al., 2011b)

Sample Label	Area	Coordinates ^(a)		H ₂ O	CO ₂	H ₂ S	H ₂	CH ₄	O ₂	N ₂
		ISN93 East	ISN93 North							
RED-001	Reykjadalur	390876	396240	990600	3665	130	45.0	26.9	16.3	7.32
RED-002	Reykjadalur	391584	396348	989900	3410	333	45.0	1.12	4.50	5.29
RED-003	Reykjadalur	391862	396155	990800	3632	67.6	54.0	1.12	10.1	5.88
RED-004	Reykjadalur	391594	395380	985200	4362	217	72.0	1.12	407	147
RED-005	Reykjadalur	391543	395042	982600	6915	205	135	1.12	2.25	5.98
RED-006	Reykjadalur	391122	394788	990200	3812	75.0	9.00	1.12	22.5	13.0
GRD-044	Grændalur	392747	395596	994900	19.8	0	45.0	10.1	116	0.05
GRD-010	Grændalur	391906	393381	996100	2614	62.3	54.0	8.98	3.38	2.62
GRD-038	Grændalur	392109	393564	995600	1700	83.4	63.0	1.12	2.81	3.26
GRD-007	Grændalur	392186	393000	994800	1927	91.3	72.0	3.37	11.8	15.4
GRD-008	Grændalur	392750	393554	994300	2032	173	108	5.61	9.00	17.7
GRD-012	Grændalur	392504	393673	994100	2306	25.9	99.0	3.37	5.06	9.00
GRD-014	Grændalur	392564	393915	995300	1449	86.6	18.0	1.12	106	37.8
GRD-015	Grændalur	392899	393996	993300	2524	150	171	3.37	6.19	9.00
GRD-002	Grændalur	392525	395717	987600	4921	120	27.0	1.12	6.19	4.80
GRD-003	Grændalur	392578	395971	991300	3436	98.2	36.0	1.12	9.00	6.87
GRD-004	Grændalur	392722	396201	990900	3559	124	54.0	1.12	5.06	6.77
GUD-001	Gufudalur	392924	390490	995600	1636	38.5	9.00	1.12	30.4	15.1
GUD-005	Gufudalur	393140	391052	997700	870	42.2	9.00	0.00	2.25	2.03
GUD-003	Gufudalur	393425	391171	996700	1207	48.0	9.00	1.12	16.9	12.0
GUD-002	Gufudalur	393377	391699	996400	1402	67.0	9.00	1.12	2.81	3.91
GUD-002L	Gufudalur	393608	392329	997100	1107	51.2	0.00	0.00	7.31	3.21
GUD-003G	Gufudalur	393837	393188	994500	2231	0	18.0	0.00	3.38	0.30
GUD-003H	Gufudalur	393875	393396	994200	2241	115	18.0	3.37	2.81	6.38
GUD-006F	Gufudalur	394194	394485	992900	2864	49.6	0	0.00	1.69	1.19
GUD-006G	Gufudalur	394216	394145	994900	1983	84.5	9.00	1.12	4.50	4.01

^(a) The coordinates were obtained through georeferenced maps from the report using QGIS v.3.20 software

Supplement 2: Chemical comp. of thermal waters from previous studies

Table S2. The chemical composition of thermal waters in Iceland. (Stefánsson et al., 2016a)

Sample #	Location	Area	Type	Coordinates	Date	Temp °C	pH	°C	SiO ₂ [ppm]
81-3018	Hveragerði	Hveragerði	sp		24/06/81	12	7.57	24	31.7
02-201	Hveragerði, neðan við foss	Hveragerði	sp	64.0006	01/01/02	90	7.57	23	161
02-202	Hveragerði, neðan við foss	Hveragerði	sp	64.0015	01/01/02	100	9.34	24	182
02-203	Hveragerði, við sundlaug	Hveragerði	sp	64.0025	01/01/02	100	9.41	23	252
02-204	Hveragerði, við borholu nr. 3	Hveragerði	sp	64.0090	01/01/02	65	7.36	23	92.3
02-205	Hveragerði, við B&B Frosti og Funi	Hveragerði	sp	64.0035	01/01/02	99	9.52	24	287
02-206	Bóluhver	Hveragerði	sp	64.0040	01/01/02	98	9.64	24	264
02-207	Bóluhver, ofan við hverinn	Hveragerði	sp	64.0040	01/01/02	99	8.82	24	200
02-208	Bóluhver, niðri við ána	Hveragerði	sp	64.0040	01/01/02	100	7.30	24	150
02-209	Hveragerði, við borholu nr. 8	Hveragerði	sp	64.0151	01/01/02	75	6.69	24	128
02-210	Hveragerði, uppspretta inni í bænum	Hveragerði	sp	64.0007	01/01/02	92	9.24	23	314
02-211	Hveragerði, uppspretta inni í bænum	Hveragerði	sp	64.0009	01/01/02	67	9.22	24	290
05-024	Hveragerði	Hveragerði	rs	64.0137	01/01/05	11	7.52	21	20.7
05-025	Hveragerði	Hveragerði	rs	64.0113	01/01/05	7	7.92	22	15.3
05-026	Hveragerði	Hveragerði	rs	64.0117	01/01/05	7	7.86	22	14.6
07-3706	Hveragerði, við laxastiga	Hveragerði	sp	64.0097	12/07/07	61	9.60	17	271
07-3707	Hveragerði, við laxastiga	Hveragerði	sp	64.0097	12/07/07	53	9.55	22	265
07-3708	Hveragerði, við laxastiga	Hveragerði	sp	64.0097	12/07/07	65	9.65	17	273
07-3710	Hveragerði, við á	Hveragerði	sp	64.0097	12/07/07	69	7.74	18	150
07-3711	Bóluhver	Hveragerði	sp	64.0040	12/07/07	101	9.60	22	279
09-ÁKS-12	Ölkelduháls	Ölkelduháls	sp	64.0567	12/06/09	70	6.60	19	196
09-ÁKS-13	Ölkelduháls	Ölkelduháls	sp	64.0567	12/06/09	70	6.52	21	195
AS14	Ölkelduháls, svört laug	Ölkelduháls	sp	64.0567	1/1/12	70	6.23	21	195
AS15	Ölkelduháls, við svarta laug	Ölkelduháls	sp	64.0567	1/1/12	70	6.59	21	196
14-SLL-01	Hveragerði	Hveragerði	sp	64.0020	13/05/14	69	7.44	22	180
14-RSA-30	Hveragerði	Hveragerði	sp	64.0066	08/09/14	98	2.53	22	170
14-RSA-37	Hveragerði	Hveragerði	sp	64.0066	08/09/14	76	2.25	22	263
15-HEN-01	Grænsdalur	Grænsdalur	sp	64.0305	21/05/15	97	9.15	23	140
15-HEN-02	Grænsdalur	Grænsdalur	sp	64.0309	21/05/15	94	8.51	23	129
15-HEN-03	Grænsdalur	Grænsdalur	sp	64.0031	21/05/15	89	8.45	23	128

Table S2. (... Continuation) The chemical composition of thermal waters in Iceland.
(Stefánsson et al., 2016a)

Sample #	B [ppm]	Na [ppm]	K [ppm]	Ca [ppm]	Mg [ppm]	Al [ppm]	Feror [ppm]	Cl [ppm]	F [ppm]	CO ₂ [ppm]	SO ₄ [ppm]	H ₂ S [ppm]
81-3018	0.020	14.6	1.22	7.12	3.00			16.8	0.050	41.6	10.0	< 0.01
02-201	0.342	115	4.82	8.53	0.308	0.022	0.047	76.5	1.20	122		2.68
02-202	0.354	144	5.34	1.35	0.024	0.138	<0.02	84.0	1.29	102		1.41
02-203	0.539	162	7.74	1.67	0.003	0.262	<0.02	148.7	2.06	50.0		3.97
02-204	0.173	68.8	3.42	14.0	1.09	0.009	<0.02	36.2	1.07	99.9		1.54
02-205	0.577	169	10.3	2.05	0.006	0.420	<0.02	160.7	2.29	39.7		7.18
02-206	0.502	156	9.17	1.84	0.003	0.479	<0.02	135.8	1.91	24.2		8.52
02-207	0.331	132	7.29	1.80	0.037	0.200	0.027	86.2	1.35	88.7		3.36
02-208	0.169	94.4	6.30	10.2	0.857	0.021	<0.02	38.3	0.807	136		2.20
02-209	0.064	83.3	6.10	34.1	9.89	0.007	<0.02	14.9	0.383	346		0.751
02-210	0.582	173	10.9	1.87	0.023	0.271	<0.02	166.0	2.30	59.6		2.39
02-211	0.571	161	10.2	2.50	0.087	0.285	0.025	148.1	2.40	47.9		<0.010
05-024	0.004	7.69	1.12	12.5	5.63	0.000		9.9		52.0		
05-025	0.007	9.51	0.670	6.02	2.37	0.006		15.1		22.7		
05-026	0.005	8.89	0.636	6.13	2.50	0.006		16.3		20.5		
07-3706	0.490	148	12.1	7.77	1.37	0.579	0.003	112	2.39	42.1	57.1	0.409
07-3707	0.488	149	12.0	8.46	1.45	0.475	0.002	112	2.34	43.5	62.8	<0.01
07-3708	0.495	150	12.2	7.35	1.26	0.606	0.002	112	2.38	40.2	53.4	1.43
07-3710	0.247	108	4.26	20.0	3.22	0.078	0.010	39	1.29	121	37.0	0.374
07-3711	0.575	173	11.6	2.49	0.012	0.320	0.015	131	2.59	20.2	70.8	4.12
09-ÁKS-12	0.010	19.8	2.61	42.2	10.2	0.007	0.013	5.20	0.021	204	35.6	0.007
09-ÁKS-13	0.010	19.1	2.28	41.3	11.8	0.008	0.018	5.28	0.027	258	12.3	0.007
AS14	0.01	19.0	2.28	41.3	11.8	0.01	0.02	5.28	0.03	12.3	258	0.01
AS15	0.01	20.0	2.61	42.2	10.2	0.01	0.01	5.2	0.02	35.6	204	0.01
14-SLL-01	0.261	110	5.07	6.92	0.418	0.021	<0.005	42.1	1.26	118	45.8	1.55
14-RSA-30	0.138	5.50	0.531	25.5	12.2	34.3	12.4	7.62	0.254	13.3	419	<0.01
14-RSA-37	0.104	6.84	2.25	16.2	11.3	35.4	20.1	1.21	0.242	4.25	632	<0.01
15-HEN-01	0.015	58.6	4.13	3.47	0.067	0.183	0.018	8.43	0.404	66.1	41.3	2.06
15-HEN-02	<0.015	37.9	4.23	27.7	1.50	0.060	<0.005	10.3	0.082	117	26.0	
15-HEN-03	<0.015	37.8	3.99	23.8	1.08	0.057	<0.005	9.47	0.123	99.8	31.6	

Table S2. (Continuation) The chemical composition of thermal waters in Iceland.
(Stefánsson et al., 2016a)

Sample # (cont...)	Location	Area	Type	Coordinates	Date	Temp °C	pH /	°C	SiO ₂ [ppm]
15-HEN-04	Grænsdalur	Grænsdalur	sp	64.0318	-21.1980	21/05/15	65	7.45 / 23	89.2
15-HEN-05	Grænsdalur	Grænsdalur	sp	64.0355	-21.1915	21/05/15	98	8.37 / 23	107
15-HEN-06	Grænsdalur	Grænsdalur	sp	64.0415	-21.1937	21/05/15	95	7.61 / 23	46.0
15-HEN-07	Grænsdalur	Grænsdalur	sp	64.0417	-21.1936	21/05/15	78	3.05 / 23	36.8
15-HEN-08	Grænsdalur	Grænsdalur	sp	64.0283	-21.1991	21/05/15	99	8.22 / 23	120
15-HEN-09	Grænsdalur	Grænsdalur	sp	64.0281	-21.1992	21/05/15	84	7.90 / 23	112
15-HEN-10	Grænsdalur	Grænsdalur	sp	64.0283	-21.1991	21/05/15	78	7.68 / 23	102
15-HEN-11	Grænsdalur	Grænsdalur	sp	64.0289	-21.1971	21/05/15	97	8.22 / 23	56.6
15-HEN-12	Grænsdalur	Grænsdalur	sp	64.0291	-21.1970	21/05/15	80	7.39 / 23	74.7
15-HEN-13	Grænsdalur	Grænsdalur	sp	64.0290	-21.1972	21/05/15	79	7.09 / 23	68.5
15-HEN-14	Grænsdalur	Grænsdalur	sp	64.0394	-21.1945	21/05/15	93	2.78 / 23	138
15-HEN-15	Grænsdalur	Grænsdalur	sp	64.0300	-21.1979	21/05/15	97	3.20 / 23	95.0
15-HEN-16	Grænsdalur	Grænsdalur	sp	64.0307	-21.1985	21/05/15	50	2.52 / 23	101
15-HEN-17	Grænsdalur	Grænsdalur	sp	64.0309	-21.1982	21/05/15	82	2.46 / 23	112
15-HEN-21	Reykjadalur, hver	Reykjadalur	sp	64.0499	-21.2282	21/05/15	100	8.07 / 22	73.4
15-HEN-30	Reykjadalur	Reykjadalur	sp	64.0521	-21.1932	22/05/15	96	8.43 / 22	41.0
15-HEN-34	Reykjadalur	Reykjadalur	sp	64.0417	-21.1935	22/05/15	74	2.64 / 22	85.2
15-HEN-35	Reykjadalur	Reykjadalur	sp	64.0478	-21.1999	22/05/15	81	2.61 / 22	118
15-HEN-36	Reykjadalur	Reykjadalur	sp	64.0477	-21.1999	22/05/15	48	5.98 / 22	136
15-HEN-37	Reykjadalur	Reykjadalur	sp	64.0479	-21.2009	22/05/15	77	4.33 / 22	86.5
15-HEN-38	Reykjadalur	Reykjadalur	sp	64.0479	-21.2019	22/05/15	76	4.69 / 22	106
15-HEN-39	Reykjadalur, leirhver	Reykjadalur	sp	64.0456	-21.2221	22/05/15	99	4.28 / 22	63.3
15-HEN-40	Reykjadalur, heit á	Reykjadalur	sp	64.0454	-21.2213	22/05/15	82	6.34 / 22	123
15-HEN-41	Reykjadalur	Reykjadalur	sp	64.0264	-21.2120	22/05/15	97	3.55 / 22	122
15-HEN-42	Reykjadalur	Reykjadalur	sp	64.0261	-21.2119	22/05/15	52	7.27 / 22	54.0
15-HEN-43	Reykjadalur	Reykjadalur	sp	64.0252	-21.2128	22/05/15	74	7.47 / 22	129
15-HEN-49	Hvammssá	Hvergerði	rs	63.9876	-21.0952	22/05/15	5	7.84 / 22	25.0
15-HEN-50	Gljúfurá	Hvergerði	rs	63.9955	-21.1165	22/05/15	8	7.96 / 22	30.6
15-HEN-51	Hengladalsá/Varmá	Hvergerði	rs	64.0203	-21.2170	22/05/15	5	7.93 / 22	22.2

Table S2. (Continuation) The chemical composition of thermal waters in Iceland.
(Stefánsson et al., 2016a)

Sample # (Cont...)	B [ppm]	Na [ppm]	K [ppm]	Ca [ppm]	Mg [ppm]	Al [ppm]	Fe _{tot} [ppm]	Cl [ppm]	F [ppm]	CO ₂ [ppm]	SO ₄ [ppm]	H ₂ S [ppm]
15-HEN-04	<0.015	23.5	3.28	43.3	12.7	0.025	0.207	12.2	0.030	182	28.5	
15-HEN-05	0.027	31.8	4.11	21.3	1.25	0.068	0.015	8.28	0.069	82.1	30.1	
15-HEN-06	<0.015	11.3	0.871	42.1	11.2	0.106	0.010	5.86	0.107	21.0	142	
15-HEN-07	0.030	6.40	0.522	12.2	10.2	1.33	6.460	5.77	0.018		148	
15-HEN-08	0.018	32.9	2.29	7.89	0.571	0.129	0.008	8.64	0.215	34.8	41.8	0.90
15-HEN-09	<0.015	40.3	4.27	35.5	3.55	0.030	0.019	9.63	0.081	112	64.6	
15-HEN-10	<0.015	40.1	3.83	33.6	5.02	0.038	0.021	9.76	0.113	136	38.3	
15-HEN-11	<0.015	12.9	1.52	14.1	4.06	0.070	0.020	8.85	0.102	43.2	21.9	0.74
15-HEN-12	<0.015	39.1	5.76	33.6	7.19	0.026	0.016	7.42	0.064	62.8	124	
15-HEN-13	<0.015	33.2	5.13	43.0	13.8	0.012	0.097	8.46	0.069	208.1	29.9	
15-HEN-14	0.044	14.0	0.965	27.9	7.25	4.27	9.65	5.21	0.031		255	
15-HEN-15	0.115	5.60	1.02	6.77	7.10	0.830	26.6	5.62	0.065		135	0.15
15-HEN-16	0.378	8.75	2.02	4.28	8.49	17.4	89.7	10.9	0.018	0.229	578	0.38
15-HEN-17	0.206	2.18	0.730	1.00	2.13	5.31	48.0	2.13	0.014		341	0.91
15-HEN-21	<0.015	15.4	4.23	31.1	7.36	0.350	1.69	9.65	0.068	62.6	59.6	
15-HEN-30	<0.015	8.82	1.23	28.9	10.1	0.037	0.054	7.35	0.148	88.0	36.7	
15-HEN-34	0.162	5.18	0.540	18.1	16.2	7.81	37.8	4.23	0.031		344	
15-HEN-35	0.080	6.11	<0.5	13.8	7.66	4.96	18.1	9.26	0.023		249	
15-HEN-36	<0.015	9.11	1.19	21.6	4.42	0.108	0.565	10.4	0.054	5.38	64.7	
15-HEN-37	<0.015	9.86	1.17	15.8	8.66	0.079	0.800	8.72	0.065		86.1	
15-HEN-38	<0.015	15.0	2.26	20.2	10.1	0.099	2.22	5.82	0.065		117	
15-HEN-39	<0.015	9.48	1.97	16.2	7.59	0.027	0.316	7.60	0.110		84.4	
15-HEN-40	<0.015	15.0	3.14	9.42	3.77	0.043	0.155	7.37	0.722	5.00	51.7	
15-HEN-41	0.016	15.6	2.22	21.3	6.83	0.257	2.65	5.29	0.084		125	
15-HEN-42	<0.015	20.5	2.82	27.6	6.56	0.077	0.213	10.1	0.077	114	33.4	
15-HEN-43	0.045	74.6	6.48	40.9	11.4	0.011	0.037	10.4	0.212	235	9.4	
15-HEN-49	0.015	15.6	1.15	8.15	3.91	0.204	0.291	17.1	0.082	39.8	4.03	
15-HEN-50	<0.015	11.1	1.42	12.6	3.40	0.047	0.061	9.03	0.076	44.1	11.0	
15-HEN-51	<0.015	9.43	0.654	13.2	3.82	0.096	0.172	8.22	0.040	46.7	9.33	

Supplement 3: Reservoir fluid composition.

Table S3. Chemical speciation of the reservoir fluid composition

Sample	Label	Location	Date sampling	T ^(a) [°C]	pH	F ⁻ [mg/kg]	Cl ⁻ [mg/kg]	SO ₄ ²⁻ [mg/kg]	Na [mg/kg]
79-0135	HV-06	Hveragerði	28.11.79	211	7.505	0.83	145	26.4	157.18
79-0136	HV-02	Hveragerði	28.11.79	191	7.293	1.59	134	35.3	158.16
79-3032	HV-04	Hveragerði	18.07.79	199	7.072	1.75	105	39.1	146.69
81-3016	HS-06	Hveragerði	19.06.81	232	7.185	0.86	154	29.8	147.48
81-3017	HS-07	Hveragerði	19.06.81	235	6.85	0.57	173	28.9	163.78
B-95809	HS-09	Hveragerði	13.11.19	185	6.847	2.07	128	60.8	167.87
1995-5202	HE-02	Ölkelduháls	30.08.95	213	5.755	0.7	154	69.4	163.22
2006-5083	HE-20	Ölkelduháls	30.05.06	246	6.233	0.58	189	25.2	194.8
2006-5132	HE-22	Ölkelduháls	01.12.06	227	6.455	0.14	186	55.4	189.42

Sample	K [mg/kg]	Ca [mg/kg]	Mg [mg/kg]	SiO ₂ [mg/kg]	B [mg/kg]	Fe [mg/kg]	CO ₂ Total [mg/kg]	H ₂ S Total [mg/kg]
79-0135	16.6	1.02	0	351			82.1	0.46
79-0136	12.9	1.18	0	245			102	3.36
79-3032	12.7	0.84	0	270	0.6	0.01	172	5.88
81-3016	18.3	0.62	0	400	0.86	0.01	293	11.0
81-3017	19.4	0.69	0	417	0.92	0.01	347	23.3
B-95809	9.9	1.97	0.1	235	0.39	0.01	140	3.15
1995-5202	17.2	0.49	0	314			3816	32.4
2006-5083	26.6	1.62	0	458	1.43	0.04	2550	241
2006-5132	20.7	1.04	0	381	1.4	0.01	1007	52.1

^(a) Temperature estimated based on Quartz geothermometer

Supplement 4: Estimation of temperature with different gas geothermometers

Table S4. Gas geothermometers of the study area expressed in °C

Sample label	Eq. 3: CO ₂	Eq. 5: H ₂ S	Eq. 6: H ₂	Eq. 7: CO ₂ /H ₂	Average Temp	Standard deviation
ÖLK-04	301	293	297	295	297 ^(a)	3
REY-09	263	279	287	298	282 ^(a)	15
GRÆ-11	272	290	292	301	289 ^(a)	12
REY-13	268	281	287	296	283 ^(a)	12
REY-15	287	298	292	295	293 ^(a)	5
GRÆ-18	269	279	282	289	280 ^(a)	8
GRÆ-19	269	295	287	296	282 ^(b)	18
GRÆ-20	265	283	283	292	274 ^(b)	13
GRÆ-21	258	283	292	306	271 ^(b)	18
GRÆ-25	271	299	299	311	285 ^(b)	20
GUF-30	248	270	286	302	259 ^(b)	16
GUF-36	266	269	286	295	268 ^(b)	2
GUF-38	230	258	272	289	244 ^(b)	20
GUF-41	213	247	272	294	230 ^(b)	24

(a): Average and standard deviation using the CO₂, H₂S, H₂, CO₂/H₂ geothermometers (Equation 3 to 7).

(b): Average and standard deviation using the CO₂ and H₂S geothermometers (Equation 3 and 5).